



RESEARCH ARTICLE

10.1029/2023GC011077

Sedimentology of Modern Bahamian Carbonate Slopes: Summary and Update

Key Points:

- Main factors controlling Bahamian slope sedimentation are revised
- Numerous data types acquired offshore were synthesized
- Our data suggest a strong influence of platform fine-grained concentration and currents on slope sedimentation models

Correspondence to:

K. Fauquembergue,
kelly.fauquembergue@gmail.com

Citation:

Fauquembergue, K., Mulder, T., Reijmer, J., Hanquiez, V., Betzler, C., Ducassou, E., et al. (2024). Sedimentology of modern Bahamian carbonate slopes: Summary and update. *Geochemistry, Geophysics, Geosystems*, 25, e2023GC011077. <https://doi.org/10.1029/2023GC011077>

Received 7 JUN 2023

Accepted 8 JUN 2024

Author Contributions:

Conceptualization: T. Mulder, J. Reijmer, V. Hanquiez, C. Betzler, E. Ducassou, A. Recouvreur

Data curation: C. Betzler, A. Recouvreur, M. Principaud

Formal analysis: V. Hanquiez

Funding acquisition: T. Mulder, E. Poli

Investigation: T. Mulder, J. Reijmer, E. Ducassou

Methodology: T. Mulder, J. Reijmer, V. Hanquiez, E. Ducassou, A. Recouvreur, M. Principaud, S. Wilk

Project administration: T. Mulder




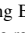
Resources: T. Mulder, J. Reijmer, E. Ducassou

Software: V. Hanquiez

Supervision: T. Mulder, V. Hanquiez, E. Ducassou, E. Poli

Validation: J. Reijmer

Visualization: C. Betzler

K. Fauquembergue¹ , T. Mulder¹, J. Reijmer^{2,3}, V. Hanquiez¹, C. Betzler⁴ , E. Ducassou¹ , A. Recouvreur¹ , M. Principaud^{1,5}, J. Borgomano^{6,7}, S. Wilk¹, and E. Poli⁷

¹UMR CNRS 5805, Université de Bordeaux CNRS Bordeaux-INP EPHE OASU, Bordeaux, France, ²Faculty of Science, Department of Geosciences, Vrije Universiteit Amsterdam, Amsterdam, the Netherlands, ³Department of Geosciences, The Netherlands and University of Fribourg/Freiburg, Fribourg, Switzerland, ⁴University of Hamburg, Hamburg, Germany, ⁵Now at Université de Brest, CNRS, Ifremer, UMR 6197, Plouzané, France, ⁶Observatoire des Sciences de l'Univers (OSU) Institut Pythéas, Centre National de la Recherche Scientifique (CNRS) (Joint Research Unit [UMR] 7330), Institut de Recherche pour le Développement (IRD) (UMR 161), Collège de France – USC INRA, Centre Européen de Recherche et d'Enseignement de Géosciences de l'Environnement (CEREGE), Aix-Marseille Université, Marseille, France, ⁷Exploration & Production SCR/RD, Total S.A., CSTJF, Pau, France

Abstract Slopes adjacent to the Bahamian carbonate platform revealed a large variety of depositional processes. In this study, we present a synthesis summarizing 109,000 km² of bathymetric and reflectivity data with ~7,900 km of seismic lines and 311 m of sediment cores that were obtained over the last 50 years. These data are used to develop a conceptual model of sedimentation patterns on Quaternary carbonate slope systems and their interaction with the adjacent shallow-water carbonate platforms. Our data highlight that during the Quaternary, factors controlling large-scale sedimentation on Bahamian slopes have numerous similarities as they have higher sedimentation rates during interglacials. At a small scale, every slope has its own characteristics that are contemporary controlled by two main characteristics: (a) facies on the adjacent shallow-water platform, and (b) the impact of shallow- and deep-water currents. Large-scale tectonics influence sediment deposition as it determines the position of the islands and impacts platform facies distribution.

Plain Language Summary The factors that allow sediment to be exported from carbonate platforms to the deep-sea need discussion. To gain a better understanding of the processes involved, the sedimentary archives of the slopes connected to these carbonate platforms are consulted. The sediments encountered vary and range from grains finer than 20 μm to coarse sandy sediments, a few millimeters in size. To understand the different processes that export those different types of sediment, we analyze various slopes of the Bahamas, a well-known pure carbonate platform system. We used both numerical data (bathymetry, reflectivity, seismic) and sediment samples from this area and compared those records for the different Bahamian slopes. We highlighted that every slope displays a different sediment record; for every slope transect the adjacent platform facies together with deep-sea processes (currents) determine the sediment distribution. The processes that export and transport the sediments are of equal importance.

1. Introduction

Bahamas is an isolated carbonate system, which constitutes one of the best-studied modern pure carbonate systems besides the Maldives. The Bahamian shallow-water platform and the surrounding Pleistocene/Holocene slope deposits have been studied by numerous research teams since the 1970s using acoustic data and samples collected by grab samplers, Küllenberg cores, and drilled cores (e.g., ODP, IODP expeditions). Some studies focused on platform facies distribution (Ball, 1967; Enos, 1974; Harris et al., 2015; Kaczmarek et al., 2010; Reijmer et al., 2009; Purdy, 1963a, 1963b), highlighting that fine-grained sediments are frequent in protected areas near islands as coarse grained sediments are mainly concentrated along the edge of the margin platform.

Other studies investigated processes associated with sediment supply to the slopes. Aforementioned studies also showed the variability in sediment production, transport and deposition of individual Bahamian regions for the Quaternary (Figure 1), which are (a) the Little Bahama Bank (LBB) slope and basin where platform export is limited to a few tens of kilometers offshore of the northern LBB margin and mostly concentrated within an Holocene wedge located at the uppermost slope (Fauquembergue et al., 2018; Mulder et al., 2017; Rankey & Doolittle, 2012). This sediment distribution highlights the impact of contouritic processes within the middle and

© 2024 The Author(s). Geochemistry, Geophysics, Geosystems published by Wiley Periodicals LLC on behalf of American Geophysical Union.

This is an open access article under the terms of the [Creative Commons Attribution-NonCommercial-NoDerivs License](#), which permits use and distribution in any medium, provided the original work is properly cited, the use is non-commercial and no modifications or adaptations are made.

Writing – original draft: J. Reijmer, E. Ducassou
Writing – review & editing: T. Mulder, J. Reijmer, C. Betzler, A. Recouvreur, M. Principaud, S. Wilk, E. Poli

lower slope environments (Chabaud et al., 2015; Fauquembergue et al., 2023; Mulder et al., 2018; Tournadour et al., 2015). Sediment deposited during glacial intervals can locally be dominated by grain support-supported, cemented debris (Lantzsch et al., 2007); (b) in Exuma Sound the slopes and basin are fed by coarse platform-derived sediments that are also transferred to the abyssal plain (Cartwright, 1985; Droxler, 1984; Le Goff et al., 2021; Reijmer et al., 1988); (c) The Tongue of the Ocean, which is a semi-enclosed basin with a high percentage of gravity-induced sediment input besides open ocean input (periplatform ooze; Droxler & Schlager, 1985; Haak & Schlager, 1989). (d) The western margin of Great Bahama Bank (GBB) on which sedimentation is marked by a significant input of fine-grained platform-derived sediments when the platform is flooded that can lead to the development of channel-levees systems (Mulder et al., 2014). Within the deeper part of the slope, the fine-grained sediments are redistributed by contourite currents (Betzler et al., 2014). Sea-level lowstand deposits are characterized by coarser grained sediment, but less abundant productivity as platforms are not flooded (Busson et al., 2019).

Previous results obtained along these slopes suggest a distinct complexity hampering the creation of a single depositional and facies model for the Bahamian slopes. Each Bahamian slope section appears to reflect the response to a specific set of variables with an explicit impact. The factors involved are (a) grain size variations in sediment input from the platform, (b) sediment redistribution through currents, (c) inherited morphology, (d) sea-level variations, (e) diagenetic processes, and (f) microbial binding.

In this manuscript, a synthesis of the studies that have been carried out on the Bahamian shelves and slopes up to now will be discussed. The study aims to: (a) combine all available acoustic and sediment data and (b) evaluate the main factors that control the development through time of the modern Bahamian slopes, and (c) determine which factors relate to the differences in sediment distribution and slope morphology for the different Bahamian slope transects.

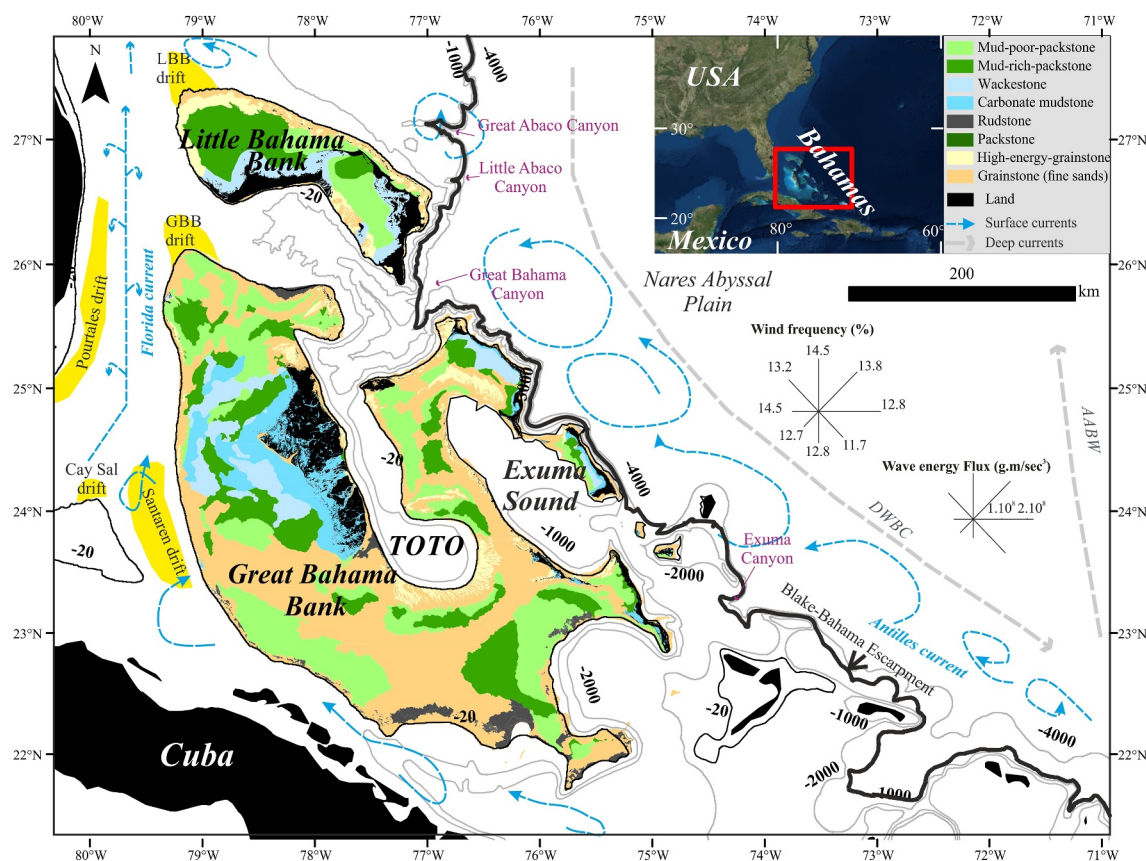


Figure 1. Physiographic map of the Bahamas showing the sedimentary facies on the shallow-water platform and the trajectory of surface and deep currents. Platform facies were established according to Purdy (1963a, 1963b), Enos (1974), Bourrouilh-Le Jan (1990), Reijmer et al. (2009), Harris et al. (2015) and Purkis et al. (2019). TOTO = Tongue of the Ocean. From Fauquembergue et al. (2023). AABW = AntArctic Bottom Water, DWBC = Deep Western Boundary Current.

2. Geological Setting

2.1. Bahamas Morphology

Bahamas are an archipelago consisting of more than 700 islands dispersed along the various isolated carbonate platforms. Two platforms are particularly large: the GBB (~108,000 km²; Figure 1) and the LBB (~17,000 km²; Figure 1). These platforms are intersected by deep basins such as the Tongue of the Ocean (TOTO), Exuma Sound, and the Columbus Basin (Figure 1), and deep canyons such as the Exuma Canyon, the Great Bahama Canyon (GBC; Figure 1) as well as the Great Abaco and Little Abaco canyons (GAC, LAC, respectively; Figure 1). These giant incisions are related to rifting activity associated with the dislocation of Pangea (Masferro et Eberli, 1999; Wylie Poag, 1991). Both the platform and canyon positions and their development are structurally controlled (Andrews et al., 1970; Mulder et al., 2018; Recouvreur et al., 2020).

2.2. Hydrodynamics

Different currents surround and interact with the Bahamian platforms. They include two northward-directed surface currents: the Florida and the Antilles current (<1,000 m water depth; Figure 1), which join at the north-western tip of the LBB to form the Gulf Stream. The Antilles current consists of different branches that border the north, the east, the south and south-west of the Bahamas. The Florida current circulates around Cay Sal Bank and borders the north-western GBB and western LBB (Bergman et al., 2010; Betzler et al., 2014; Lüdmann et al., 2016). Along the western margin, the Deep Western Boundary Current (DWBC) flows southward along the Blake Bahama Escarpment at water depths of >1,000 m (Figure 1; Leaman et al., 1995; Lüdmann et al., 2016).

2.3. Distribution of Platform Facies

Carbonate productivity and associated carbonate sedimentation vary across the Bahamian platforms; hence, the platforms display a very diverse facies distribution pattern (Enos, 1974; Harris et al., 2015; Purkis et al., 2019; Reijmer et al., 2009). On the LBB, green algae such as *Halimeda*, *Penicillus* and *Nhipocephalus* produce a large amount of the bank mud present within the lagoon. As illustrated in Figure 1, mud is predominant on the leeward side of the islands and in parts of the interior where it is protected from high hydrodynamic processes such as winds and swell. Purdy (1963a, 1963b) and Enos (1974) highlighted the large amount of mud present on the GBB and LBB platforms as other studies showed that for example, on GBB facies varied depending on the location on the platform in response to variations in wind and current intensities (Bourrouilh-Le Jan 1990; Reijmer et al., 2009; Harris et al., 2015; Purkis et al., 2019; Figure 1). Coarser sediments, such as grainstones, dominate the edges of the platforms (Figure 1) as various hydrodynamic processes such as storm-induced currents, shallow currents and tides remove the mud (Harris et al., 2015; Purkis et al., 2019).

2.4. Bahamian Slope Deposits

Modern sediment deposition on the slope surface relies on two processes:

1. Sediment export from the platform to the slope. Sediment transfer preferentially occurs when the platforms are flooded (Glaser and Droxler, 1991; Schlager et al., 1994), and mainly when winter cold fronts pass by Bustos-Serrano et al. (2009), Dierssen et al. (2009), Purkis et al. (2017), Wilson and Roberts (1992, 1995), and Yao et al. (2023) as these cold fronts produce dense waters that are able to transport sediments, a process called “density cascading.” Other sediment transport events occur in the aftermath of hurricanes (Boss & Neumann, 1993; Fauquembergue et al., 2018; Toomey et al., 2013). Tidal flushing helps in mobilizing fine-grained material during both meteorological events (Fauquembergue et al., 2018; Lopez-Gamundi et al., 2023; Mulder et al., 2017). On the slopes, platform sediment export is structurally observed within sedimentary structures like large dissolution depressions acting today as plunge-pools (Mulder et al., 2019), sediment waves and gullies (Betzler et al., 2014; Mulder et al., 2014, 2017; Recouvreur et al., 2020; Schnyder et al., 2018; Wunsch et al., 2016), but also with contourite deposits (Eberli & Betzler, 2019; Mulder et al., 2019).
2. Sedimentation related to current circulation. Some carbonate mounds, scours and current-related lineaments are observed on the middle to lower slopes of both LBB (Tournadour, 2015) and GBB (Correa et al., 2012; Lüdmann et al., 2016; Principaud, 2016). Current circulation allows the development of five carbonate contourite drifts along the Bahamian slopes (Figure 1) detailed by Bergman (2005) and Mullins et al. (1980) being the: (a) Pourtales Drift which is an asymmetric separated-detached drift (>24,000 km² and 1 km thick),

(b) the Cay Sal detached drift (20 km in length and 300 m thick), (c) Santaren Channel confined drift (9,600 km² and 600 m thick), (d) Great Bahama detached drift (>150 km in length and 500 m thick), and (e) the LBB plastered drift (3,000 km² and 500 m thick; Mullins et al., 1980) which fills a slide scar (Chabaud et al., 2015; Tournadour et al., 2015). The contourite drift deposits were also detailed in Eberli and Betzler (2019) and Mulder et al. (2019). Along the Blake Bahama Escarpment, another small detached drift (Mulder et al., 2019) made of mixed carbonate and hemipelagic sediments (Cartwright, 1985; Droxler, 1984) is formed by the DWBC.

Schlager and Ginsburg (1981) and Adams and Kenter (2013) discussed that Bahamian slope angles help in recognizing the main gravity processes that occur on slopes (Figure 2): (a) accretionary slopes on gentle slopes lead to slumps and gravity flows, (b) by-passing slopes with intermediary angles lead to turbidites with hard-ground gullies, as (c) erosional slopes lead to turbidity and contour currents confined within slopes and deep basins. They also stated that the difference between windward and leeward exposure of a slope may have an impact on slope morphology, as depositional slopes are mainly found on the western flanks of LBB and GBB as wind the trade winds mostly come out of the north-east to east. Bottom current velocity can also have an impact on the deposition/erosion of a slope. This study demonstrates that the Schlager and Ginsburg (1981) model needs to be re-evaluated.

3. Data and Methods

3.1. Acoustic Data

A total of ~109,000 km² of bathymetry and backscatter data (Table 1; Figures 2 and 3) and 7,894 km of Very High-Resolution vertical seismic lines (VHR; 3.5 kHz; Table 1; Figure 4) were analyzed. Acoustic data were used to determine the slope structures and morphologies independently of data discussed in various studies (Bergman, 2005; Bergman et al., 2010; Betzler et al., 2014; Mulder et al., 2014, 2017, 2018; Principaud, 2015; Recouvreux, 2017; Recouvreux et al., 2020; Tournadour, 2015; Wunsch et al., 2016). In this study, we used ArcGIS software (Esri; version 10.6) to combine, evaluate and summarize all data. The total data set provides a synthesis of sedimentation processes at a Bahamian-wide scale (Figure 4).

Data are derived from a variety of sources and therefore rely on data sets with different scales and with varying resolution, as presented in various studies. Some of the data were acquired by high-resolution acoustic tools (Table 1), whereas TOTO and Exuma Sound bathymetry were digitized from published data (Cartwright, 1985; Crevello & Schlager, 1980; US Naval Oceanographic Office, 1967). The latter are marked as “low resolution” data in Table 1. Therefore, it is important to note that some small-size structures (sediment waves, small size channel levee system etc...) could only be highlighted in those areas with sufficient data resolution, as others will remain hidden until new acoustic data become available.

3.2. Sediment Samples

In total, 311 m of sediments, obtained by gravity cores and grabs, were used to detail the sedimentation processes on the Quaternary slopes and to classify the sediments present (Table 2; Figures 5–7).

The gravity cores collected on the slope were used to characterize the present-day slope facies and Bahamian Quaternary sedimentation patterns through time. The cores (see detailed cruises and bibliography in Table 1) analyzed by Droxler (1984; GAC abyssal plain area cores), Cartwright (1985; Exuma canyon area cores), Chabaud et al. (2015; northwestern LBB slope cores), Chabaud (2016, northwestern LBB and western GBB slopes cores), Fauquembergue et al. (2023; northeastern LBB slope) and Fauquembergue et al. (2018; uppermost LBB slope cores) were used in this evaluation. The sandy fraction established for this study is based on grain-size measurements using a laser particle size analyzer (Malvern Mastersizer 2000). Sand size fraction of surface sample descriptions published by US Naval Oceanographic Office (1967) in TOTO were also incorporated in the study.

A first summary of combined GBB and LBB facies was discussed by Principaud (2016) based on Ball (1967), Enos (1974), Reijmer et al. (2009), Kaczmarek et al. (2010), Harris et al. (2015) and Purkis et al. (2019). Data collected before the 2000s are based on samples, while data acquired more recently are based on remote sensing acquisitions. In this new study, facies recognized in cores collected on the northern GBB by Bourrouilh-Le Jan (1990) were also included as they were not used in previous studies.

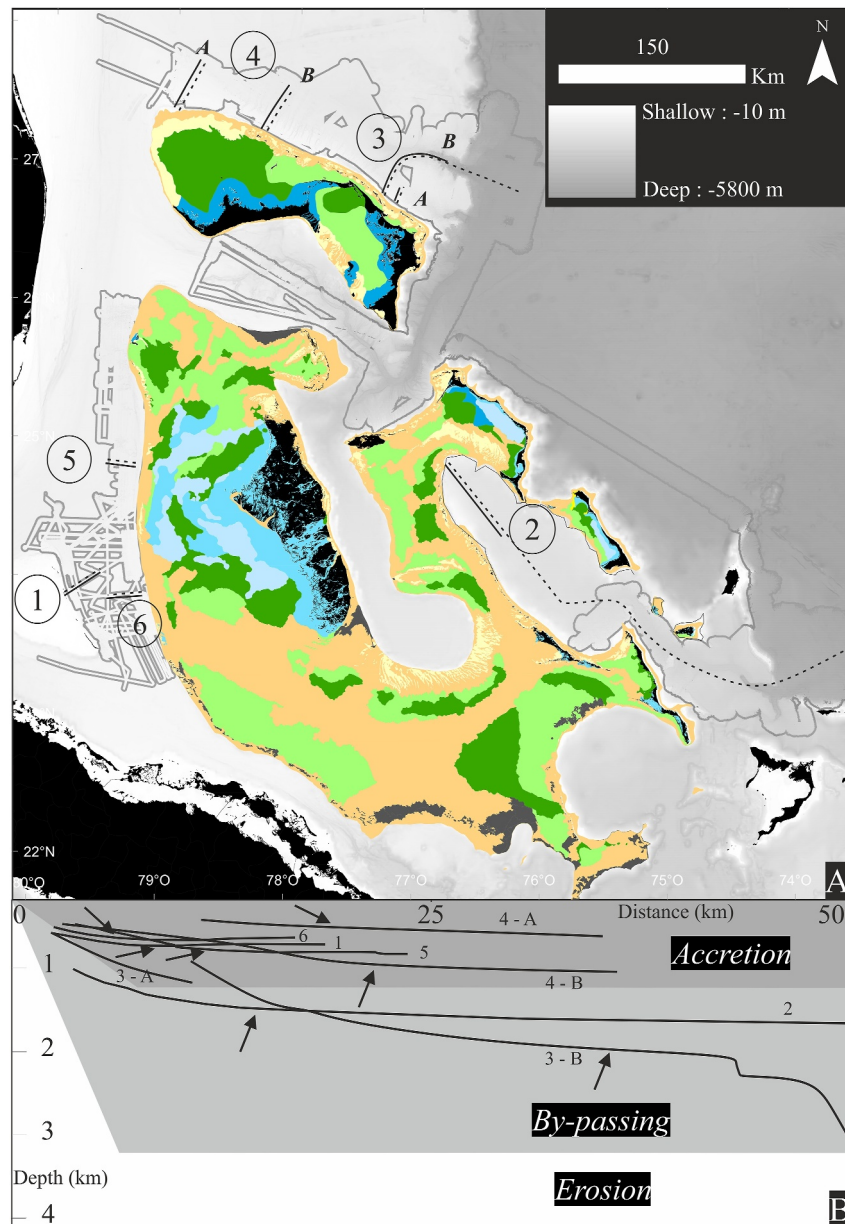


Figure 2. (a) Synthesis of Bahamian slope bathymetry. Data acquired onboard with a resolution higher or equal to 50 m (see Table 1) are outlined in black and superposed on GEBCO data (GEBCO Bathymetric Compilation Group, 2020). Platform facies were established according to Enos (1974), Bourrouilh-Le Jan (1990), Reijmer et al. (2009), Harris et al. (2015), and Purkis et al. (2019), see Figure 1 for platforms facies legend. Solid lines indicate the location of (b) bathymetric profiles as dashed lines indicate the location of models shown in Figure 7. (b) New bathymetric profiles compared to the Schlager and Ginsburg (1981) model indicating the type of slope concerned. Arrows indicate the approximative location of the break in slope where it tends to flatten.

4. Results

4.1. Bathymetry

The combined bathymetric map allows a direct comparison of the individual slope profiles across the Bahamian archipelago (Figure 2b). Slope profile analysis highlights that at distances between 10 and 20 km away from the platform margins, every slope tends to flatten. This slope break appears closest to the shelf break in the Santaren Channel and the Florida Strait (<10 km), as it is located at ~15 km in Exuma Sound and even further at over 18 km on the northern LBB slope. The slope flattening occurs at different water depths: less than 1,000 m water

Table 1
Summary of Acoustic and Sedimentary Data Considered for This Study

Cruise	Tools	Resolution	Surface/Length of seismic line/Meters of cores collected	Acquired data	Processing software	Non-exhaustive list of previous references using the data set
Bacar (1981) (Vincent, 1981)	16 sea beam acquisition	Low	24,773 km ²	Bathymetry	Caraiibes and ArcGIS Desktop	(Cartwright, 1985; Droxler, 1984)
GEBCO	Küllenberg corer		128 m	Cores		
NAVY property	Combination of available data	±400 m				
PAT0503 (2003)	Unknown	Low	12,116 km ²	Bathymetry	ArcGIS Desktop	
AT07L30, (2003)	Simrad EM121	±20 m	32 samples	Surface samples		
RB0301 (2003)	SeaBeam 2112 multibeam echosounder	±50 m	1,786 km ²	Bathymetry	Caraiibes	
KN182L02 (2005)	SeaBeam 2112 multibeam echosounder	±50 m	5,588 km ²	Backscatter	MBSytem	
RB1201 (2012)	SeaBeam 2112 multibeam echosounder	±50 m	1,916 km ²	Bathymetry	Caraiibes	
M95 CJCARB (2013) (Betzler & Reijmer, 2014)	SeaBeam 2112 multibeam echosounder	±50 m	3,674 km ²	Backscatter	MBSytem	
Carambar 1.5 (2014)	Kongsberg EM122 multibeam echosounder	±50 m	3,131 km ²	Bathymetry	Caraiibes	
	ATLAS PARASOUND P70 echosounder	±10 m	3,700 km ²	Backscatter	MBSytem	(Betzler et al., 2014; Busson et al., 2019; Lüdmann et al., 2016; Wunsch et al., 2018)
	Kongsberg EM122 multibeam echosounder				ArcGIS Desktop	
	Teledyne Reson Seabat 7125 multibeam echosounder	±5 m	147 km ²	Bathymetry	Caraiibes and ArcGIS Desktop	(Fauquembergue et al., 2018; Mulder et al., 2017; Recouvreur et al., 2020)
	Knudsen Chirp 3260 (3.5 kHz)			Backscatter	Caraiibes and ArcGIS Desktop	
	Küllenberg corer and grabs	±10 cm	1,120 km	VHR seismic	SouderSuite	
			90 m	Cores		
Carambar (2010) (Thierry, 2010)	Kongsberg EM302 multibeam echosounder	±20 m	9,379 km ²	Bathymetry	Caraiibes	(Mulder et al., 2012, 2014; Principaud et al., 2015, 2017, 2018; Tournadour et al., 2015, 2017)
	Chirp subbottom profiler (1.8–5.3 kHz)	±20 cm	2998 km	Backscatter	SonarScope	
			43 m	VHR seismic	Kingdom	
	Küllenberg corer and grabs			Cores		
Carambar 2 (2016–2017)	Kongsberg EM122/EM710 multibeam echo-sounder	±50 m	42,503 km ²	Bathymetry	Caraiibes	(Fauquembergue et al., 2023; Mulder et al., 2018; Recouvreur et al., 2020)
	Chirp subbottom profiler (1.8–5.3 kHz)	±20 cm	3,776 km	Backscatter	SonarScope	
	Küllenberg corer and grabs	±20 cm	50 m	VHR seismic	QC Subop	
				Cores		

Note. Listed are: (i) cruise, (ii) tools used, (iii) resolution, (iv) information on the seismic line, (v) data acquired, (vi) processing software, and (vii) references of published studies.

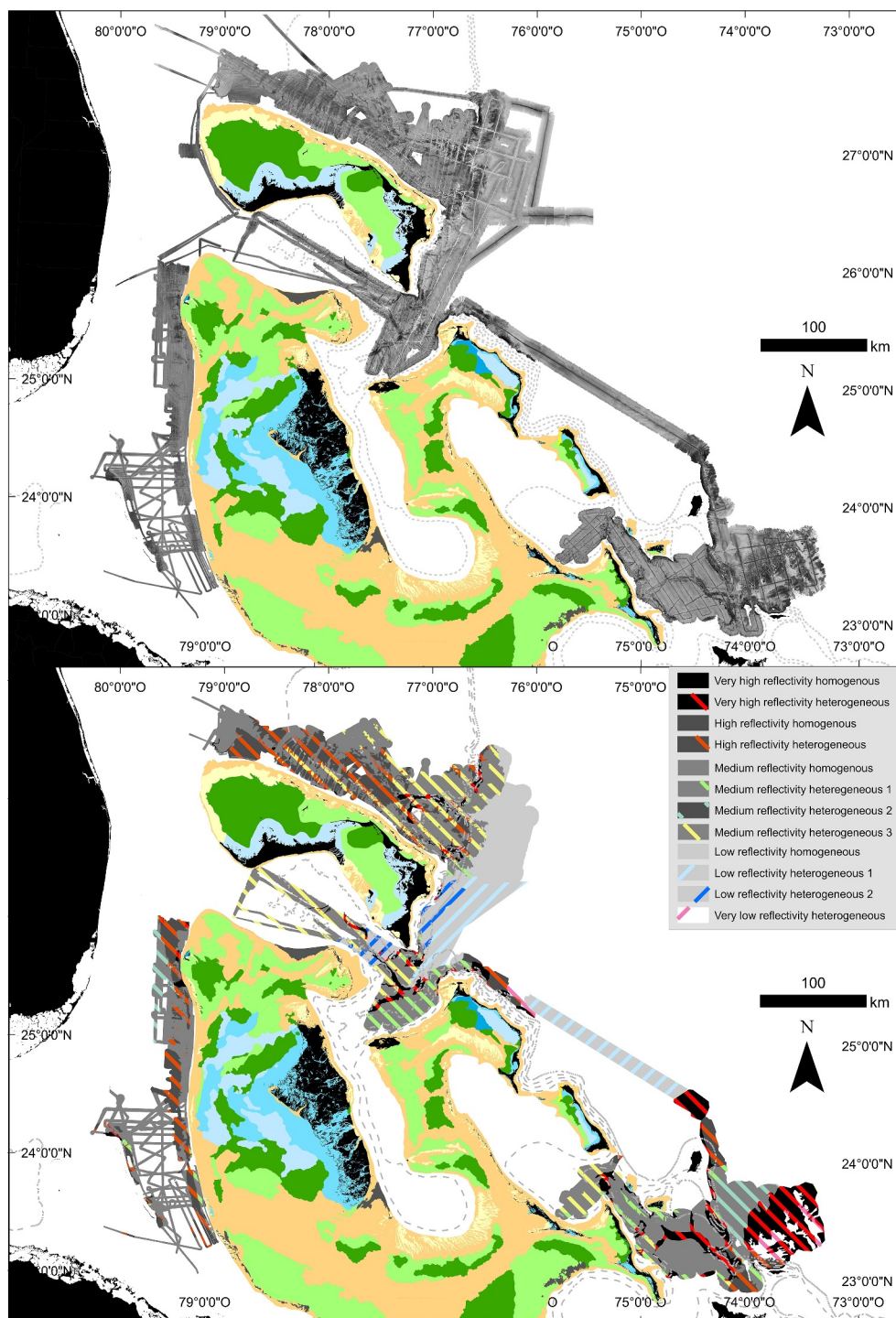


Figure 3. (a) High resolution multibeam echosounder backscatter map of the study area. (b) Distribution of acoustic facies recognized after backscatter evaluation. See Table 2 for backscatter classification, and Figure 1 for platform facies legend. Platform facies were established according to Enos (1974), Bourrouilh-Le Jan (1990), Reijmer et al. (2009), Harris et al. (2015), and Purkis et al. (2019).

depth in the Santaren Channel, the Florida Strait and the north-western LBB, which all are located on the western Bahamas and all agree with the “accretion” slope profile of Schlager and Ginsburg (1981; Figure 2). The northern Bahamian slope steepens around 1,000 m deep in the western part and at 1,200 m deep in the eastern part (Figure 2). The eastern Bahamian slopes (Great Abaco Channel and Exuma Sound; Figure 2) steepen between

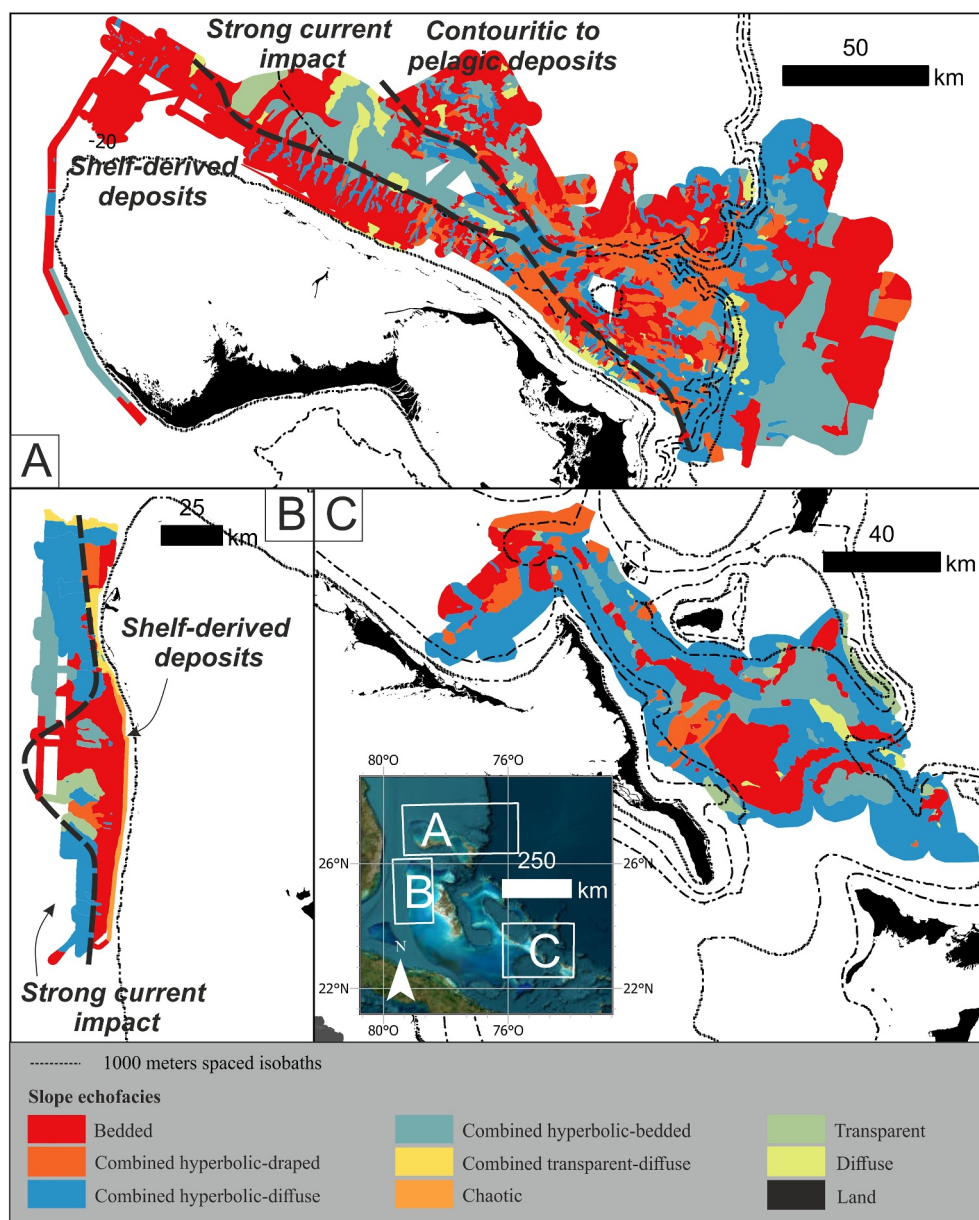


Figure 4. Echofacies map of the study area, position of seismic lines (top) and interpretations (bottom) are reported. See Table 3 for echofacies classification. Bedded and draped facies are found close to platform margins for both Northern LBB and western GBB; however, over the northern LBB, two distinct areas present deposition that is not related to the same processes (coarse grained deposition on the eastern slope). Hyperbolic-diffuse facies are predominant on Bahamian slopes. Red and orange colors are used for depositional areas, blue colors for erosional areas and green correspond to colors that we do not know.

1,500 and 2,000 m water depth and agree with a bypass model (Schlager & Ginsburg, 1981). Hence, a clear east-west variability in slope profiles can be observed; the profiles seem to steepen and reach deeper water depths when moving from west to east (Figure 2).

4.2. Reflectivity

The harmonized backscatter map (Table 2; Figure 3) shows different reflectivity's on the Bahamian slopes from low to high reflectivity, with both homogeneous and heterogeneous appearances. As those reflectivity pieces were previously analyzed in separate studies, the first inventory displayed a large variability. The main interest of the

Table 2
Classification and Description of Main Reflectivity Facies Found Along the Bahamian Slopes


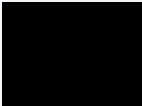
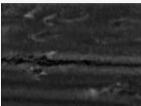

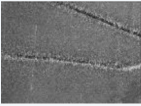

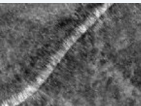

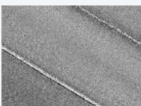

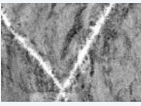
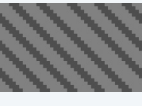






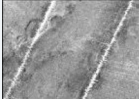

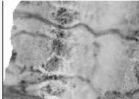

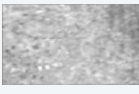

Facies	Reflectivity	Symbology (Figure 3)	Description and interpretations	Covered area (km ²)
Very highly reflective homogeneous			Very rare in the study area, this facies is generally located along some platform margins (Santaren, Samana Cay...) and within the Mass Transport Complex g scar in the northwest of LBB.	122
Very highly reflective heterogeneous			Usually found within very steep transit structures (e.g. along the Blake Bahama Escarpment) and within canyons (head of the Great and Little Abaco canyon, head and foot of the San Salvador canyon).	7,673
Highly reflective homogeneous			Minimal presence in the study area, only at the foot of the northern Eleuthera Escarpment.	172
Highly reflective heterogeneous			Frequent, generally occurring in strongly indurated sedimentary transit areas, such as gullies, tributary furrows, or landslide zones on the western slope of the LBB.	9,874
Medium reflective homogeneous			Found in areas generally subject to carbonate ooze or carbonate pelagic deposition, such as plateaus and drifts.	13,783
Medium reflective heterogeneous 1			Corresponds mainly to areas with moderately indurated gullies.	4,657
Medium reflective heterogeneous 2			Principally corresponds to areas rich in slide scars from multi-kilometer slides.	10,500
Medium reflective heterogeneous 3			Generally, corresponds to zones with furrows induced by the passage of currents.	3,258
Low reflective homogeneous			Found only in the Nares Abyssal Plain at the foot of the Great Abaco Canyon.	4,560

Table 2
Continued

Facies	Reflectivity	Symbology (Figure 3)	Description and interpretations	Covered area (km ²)
Low reflective heterogeneous			Mainly found on the Nares Abyssal Plain, probably linked to current-related structures.	5,530
Low reflective heterogeneous			Corresponds mainly to areas with weakly indurated gullies in the Great Bahama Canyon area.	1,805
Very low reflective heterogeneous			Mainly found in the Nares Abyssal Plain, both at the foot of the San Salvador Canyon and northeast of Eleuthera.	1,423

new map was to produce a map in which large-scale facies variations present on the slopes are documented; previous studies distinguished more than 20 different slope facies (Principaud, 2015; Recouvreur, 2017; Tournadour, 2015). When summarized and standardized on a large scale, the various facies classifications could be merged into a total of 12 slope facies; appearance, descriptions, and interpretations are given in Table 2.

Very low reflectivity's are always heterogeneous and can be found on the Nares abyssal plain in two areas: near north-eastern Eleuthera Island and at the base of the Exuma canyon (Table 2; Figure 3). The low reflectivity facies are homogeneous at the GAC outlet and become heterogeneous when crossing structures such as gullies at the mouth of the Little Abaco Canyon, in the Nares Abyssal Plain and in some areas that are located close to the GAC. Both medium homogeneous and heterogeneous reflectivity's are present along slopes shallower than 3,000 m and on plateaus (Table 2; Figure 3) and cover the main part of the Bahamian slopes. Homogeneous facies are related to areas related to carbonate ooze or pelagic deposits; facies become heterogeneous when they are intercepted by furrows related to currents, by slide-scars within the Blake Plateau and by more indurated gullies than those that show low reflectivity. Highest reflectivity's occur on the steepest slopes such as along escarpments (Blake Bahama Escarpment, GAC head, GBC head, Exuma head, Mass Transport Complexes [MTC] slide scar, induced gullies) and also at the outlet of Exuma canyon (Table 2; Figure 3).

4.3. Echofacies

The VHR seismic study shows the predominance of two types of echofacies: (a) bedded and (b) hyperbolic echofacies (Table 3; Figure 4). Both echofacies were recognized and classified by Principaud (2015), Tournadour (2015) and Recouvreur (2017). The bedded echofacies occur along (a) the north-eastern LBB slope, where it is dissected by various gullies, (b) the Nares Abyssal Plain, (c) the Exuma Sound area, and concentrated areas close to the platforms margins areas along both (d) the north-western LBB slope and (e) the western GBB slope (Table 3; Figure 4). Around 1,000 m deep, bedded and hyperbolic facies are usually combined with hyperbolic and diffuse reflectors. Further downslope of the latter slope areas, bedded echofacies are presently combined with hyperbolic reflectors (Table 3; Figure 4). At times, the hyperbolic echofacies occur together with bedded, undefined, or draped reflectors (Table 3; Figure 4). Hyperbolic draped reflectors are positioned only close to the GAC head (Table 3; Figure 4). Combined hyperbolic and unclear reflectors are present within most of the Exuma Sound but also occur along the western GBB where they are not affected by bedded echofacies. They also mark the steep slopes along the Blake Bahama Escarpment.

Chaotic reflectors indicate that the deposits observed do not present any internal structures (Table 3). This facies is almost absent in the study area and is only found along steep slopes like the Blake Escarpment along the northern Exuma canyon and upper slope of the western GBB (Figure 4).

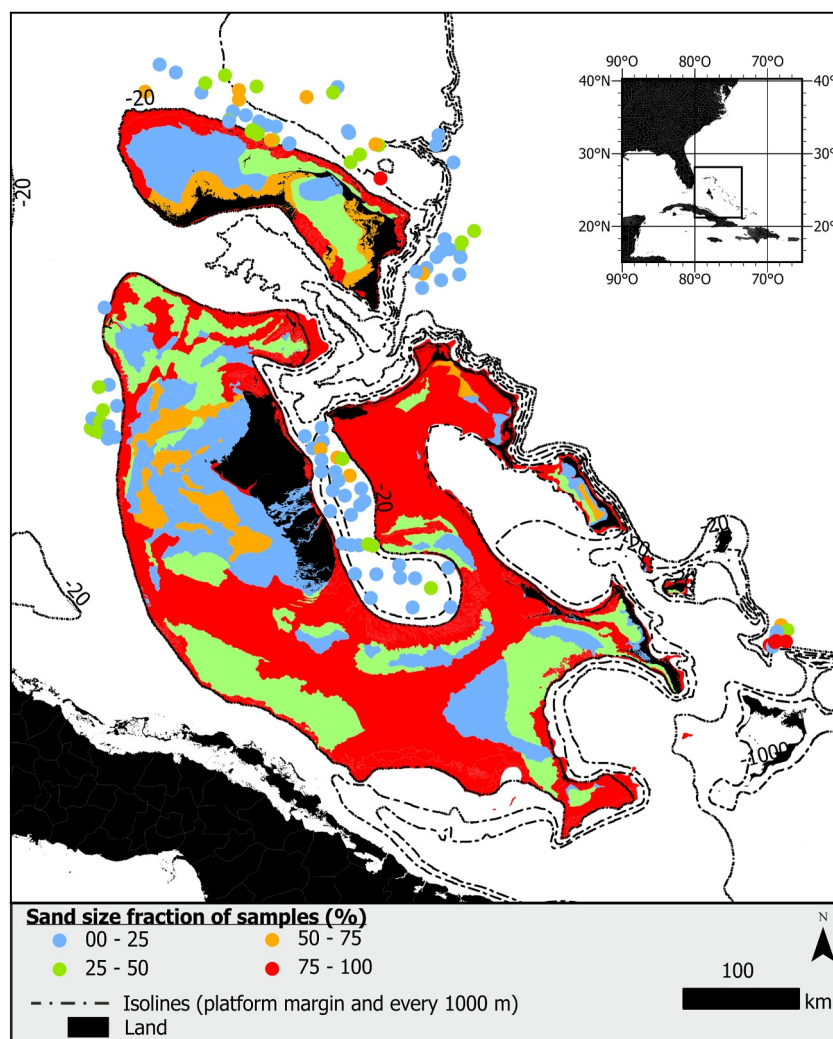


Figure 5. Results of the [% sand] analysis of Quaternary sediments presented within cores collected along Bahamian slopes. This ratio was extrapolated to the platforms facies map (Bourrouilh-Le Jan 1990; Enos, 1974; Harris et al., 2015; Purkis et al., 2019; Reijmer et al., 2009) with average sand, silt, and mud contents. Data in TOTO digitized from US Naval Oceanographic Office map (1967).

4.4. Grain-Size

The sand ratio was used to determine the variations in the distribution of coarse- and fine-grained sediment within the research area (Figure 5). The map highlights important differences in the sediment distribution within the shallow waters of the carbonate platform, along the platform margins and on the slopes. The platform facies appear to be coarser than those on the slopes, a pattern that dominates within TOTO and along the northern Bahamian margin. However, it is important to note that grain-size results for TOTO are based on surface samples and not on long core records in contrast to the other samples. These cores from the TOTO basin (Droxler, 1984; Droxler & Schlager, 1985) were not available for detailed sampling. They show that the majority of the coarse-grained turbidites were deposited during interglacial periods (Droxler & Schlager, 1985). Hence, grain-size measurements of long cores could document the amount of sand deposited during the Quaternary. A detailed sand distribution analysis highlights that coarse-grained sediments are concentrated at the outlet of the Exuma Canyon within the abyssal plain of San Salvador; sand dominates most of the samples in this area. The northern margin of the LBB also displays some, but less, areas enriched in sands, both on the north-eastern lobes and on the lower slope during Marine Isotopic Stage 5 (MIS), between 130,000 and 71,000 years ago (Fauquembergue et al., 2023; Recouvreur et al., 2020). MIS 5 is the last interglacial period before the present one. Bahamian

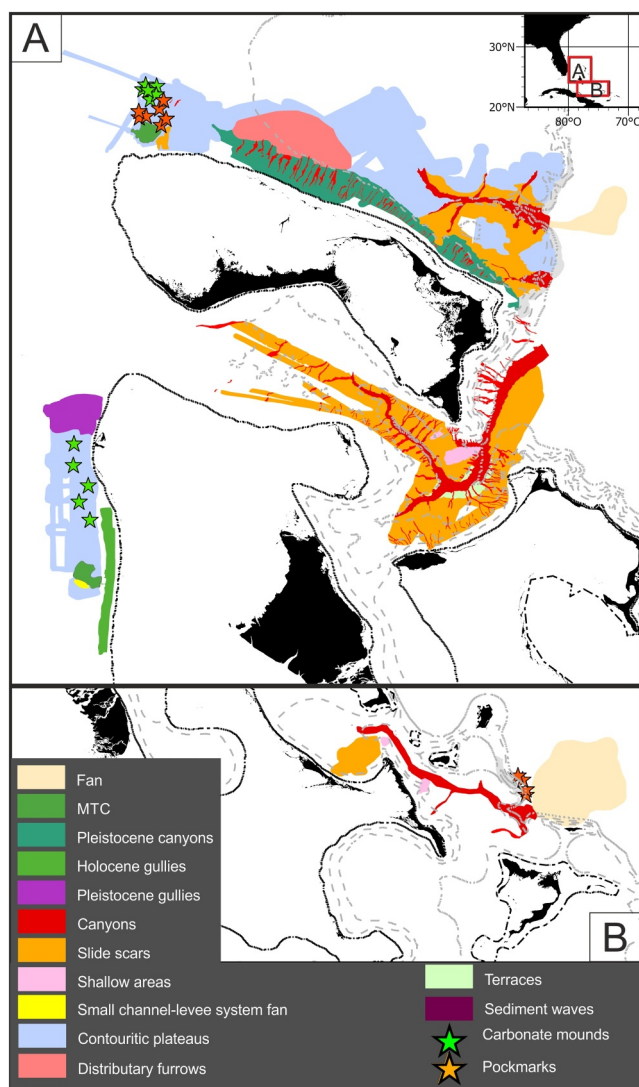


Figure 6. Synthesis of sedimentary features observed along the Bahamian slopes. Numerous canyons and gullies highlight the slope connection between shallow-water platforms and deep ocean realms. The aerial extent of hemipelagic and contour current deposition is limited and highly influenced by currents.

carbonate platform flooding can only take place during interglacial periods; thus, sediments produced on platform export to slope also. The north-western LBB slope on the MTC slide scar is slightly enriched in sand but predominantly contains carbonate ooze (Chabaud et al., 2015; Tournadour et al., 2015). Samples collected along the western GBB and at the outlets of GBC and GAC have minor quantities of sand (% < 0.25).

5. Discussion

5.1. Slope Morphology

The north-western LBB slope seems to be the continuation of the western GBB accretionary slope and the eastern Santaren slope and all display similar sedimentary features. The analysis of samples obtained at the first two sites (Figure 6) indicates that these areas are enriched in carbonate ooze. The north-eastern LBB slope, including GAC, seems to correspond to a by-pass slope similar to Exuma Sound and Exuma Canyon (Figure 2). However, sediments supplied to these canyons differ from the sediment in the GAC system and consist of fine-pelagic material partially supplied through tributaries (Fauquembergue et al., 2023). The Exuma Canyon receives fine-grained sediment (periplatform ooze) but also coarse-grained platform-derived sediments (gravity flows; Reijmer et al., 1988; Rendle-Bühning & Reijmer, 2005; Reijmer et al., 2015; Busson, 2018; Le Goff et al., 2021). These observations suggest large-scale similarities between the different canyons' morphology and strengthens the hypothesis of a structural control of these canyons rather than a sedimentary transit control on the morphology as was previously demonstrated (Recouvreux et al., 2020).

The northern LBB slope morphology agrees with the slope model evolution proposed by Schlager and Ginsburg (1981; Figure 2), with a steepening slope evolving into an erosional slope. The “erosional slope” morphology of the eastern LBB slope is shaped by the combination of turbidity currents supplying sediment to deep-water lobes, and the Antilles Current affecting the plateau located at the GAC head (Recouvreux et al., 2020). The western LBB slope displays some aspects of an “accretionary slope” with sediments accumulating especially within the MTC slide scar (Chabaud et al., 2015). However, this part of the LBB slope also contains large-scale slumps (Tournadour et al., 2015) and redistributed slope-derived sediments (Lantzsch et al., 2007); thus, the qualification of “accretionary slope” is not due to platform export but mostly by the presence of peri-platform ooze (Chabaud et al., 2015) forming the LBB drift. Overall, the slope bathymetry and observed sediment structures both agree with accretion (Figure 2). The E

to W change of the northern LBB slope morphology could be due to the regional tilting proposed by Austin et al. (1986) and Mulder et al. (2012) and/or to the imprint of GAC incision progressing structurally westward (Recouvreux et al., 2020).

Our results (Figure 2) highlight that several relative flat areas are observed along all Bahamian slopes at water depths varying between 1,000 m (western slopes) and 1,500 m (eastern slopes). Those relative flat areas are positioned deeper when moving from the northern LBB western to the eastern slope. This deepening also occurs at a larger scale as the eastern GBB flat area occurs at a shallower water depth than the those in the eastern area (Exuma slope). Thus, this Bahama-wide feature strongly suggests that tilting affected the whole Bahamas and not only the northern LBB (Harwood and Towers, 1988; Kenter, 1990). To strengthen this observation, it would be interesting to analyze the precise bathymetry of the TOTO and/or the Exuma Sound slopes. However, the accurate bathymetry along these slopes is not available, but it would be interesting to determine if the aforementioned tilt not only affected the northern LBB but also if it was a process that influenced the general morphology of all Bahamian slopes.

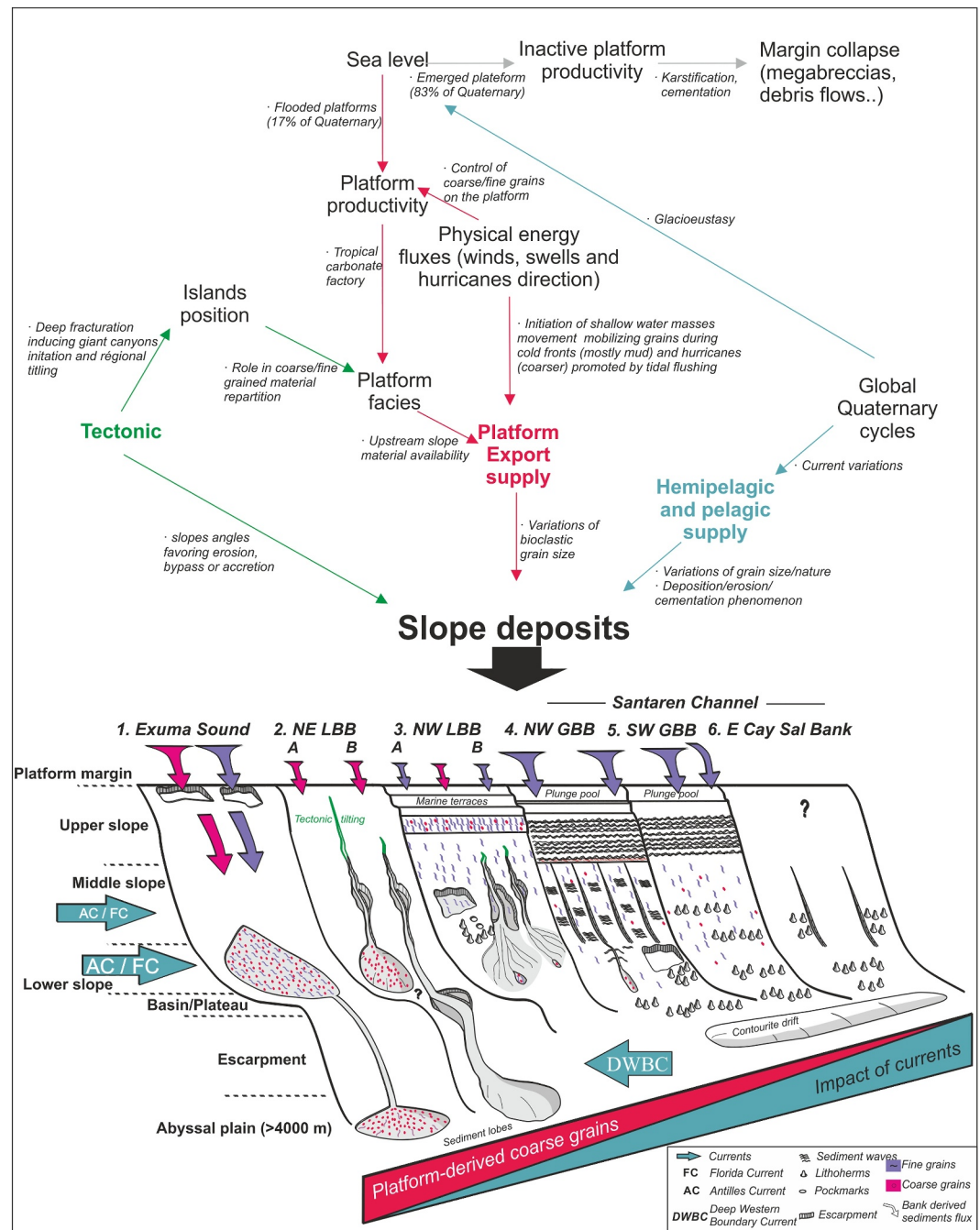
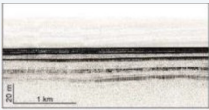
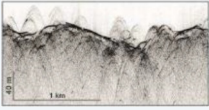
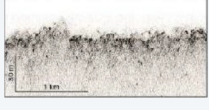
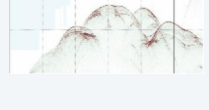



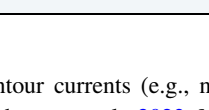


Figure 7. Global Quaternary (re-)sedimentation processes and morphology for various Bahamian slopes. Location of the individual slope profiles is provided in Figure 2.

5.2. Backscatter

The base of the Blake Bahama Escarpment (Figure 1) is draped by contourites resulting from the circulation of the DWBC (Cartwright, 1985; Fauquembergue et al., 2023). Higher on the slope, these contourites with their homogeneous reflectivity facies are incised by deep gullies (<3,000 m), which generate a heterogeneous facies distribution (Table 2; Figure 3). Zones with fine-grained carbonate deposits (ooze or pelagic carbonate) show medium homogeneous reflectivity facies. Medium reflectivity facies become heterogeneous when furrows erode deposits or when gullies become filled by moderately to strongly indurated sediments. A similar heterogeneous

Table 3
Identified Echofacies Along Bahamian Slopes With Their Individual Characteristics as Encountered in the Profiles, Shown on the Right Side of the Table by Principaud (2015), Tournadour (2015), Fabregas (2017), and Recouvreur (2017)

Echofacies	Profiles
Bedded	
Combined hyperbolic-draped	
Combined hyperbolic-diffuse	
Combined hyperbolic-bedded	
Combined transparent-diffuse	
Chaotic	
Transparent	
Diffuse	

reflectivity pattern occurs in areas where currents are intense and slightly erosive (Table 2; Figure 3). The highest reflectivity facies are found along the steep Blake Bahama Escarpment or giant canyon flanks (Table 2; Figure 3).

The reflectivity map (Figure 3) highlights three main properties of the Bahamian slopes:

1. The canyons incising the Blake Bahama Escarpment show differences at their outlets. The Great Abaco, Little Abaco and Great Bahama canyons show high reflectivity facies that is exclusively associated with their steep flanks. The reflectivity of the facies that occur in Exuma Canyon is also high at the mouth of the canyon, probably due to the presence of coarse platform-derived deposits and material failed from BBE.
2. Three types of gullies were recognized within the highly reflective heterogeneous, the medium reflective heterogeneous 1 and low reflective facies (Table 2). Reflectivity here reflects to degree of sediment induration within and around structures. (a) The first type comprises strongly indurated incisions that are mainly located in areas that are strongly affected by the passage of currents, such as in the west of GBB or in the north-western part of LBB (Table 2; Figure 3). (b) The second type includes moderately indurated gullies characterizing the southern margins of the GBC. (c) The third type contains weakly indurated gullies that mark the Blake Bahama Escarpment.
3. The reflectivity map also highlights differences between the northern margin of the LBB (windward slope) and the western margin of the GBB (leeward slope), even though the reflectivity facies are similar. The lower slope of the GBB has margin parallel furrows similar to those present at the north-western LBB, which are associated with currents (Florida current and Antilles current, respectively). However, the lower slope environment of the western GBB has higher reflectivity facies than the upper slope of the LBB. The confinement of the Florida Current along the GBB induces current speeds higher than along the LBB influenced by the Antilles Current (Johns, 2011). This difference in current speed probably explains the more intense induration of sediments of the GBB lower slope compared to the LBB slope. The high current speed in the Santaren Channel is also highlighted by the increase in coarse grain-size when moving downslope (Betzler et al., 2014) and the current shadows marking the cold-water coral mounds (Lüdmann et al., 2016).

5.3. VHR Seismic

The VHR seismic study shows the predominance of two types of echofacies: (a) the bedded echofacies and (b) the hyperbolic echofacies (Table 3; Figure 4). Two types of deposits can induce the presence of bedded echofacies (Figure 4): (a) hemipelagites or periplatform ooze resulting from sediment export from the shallow-water platform as can be found along the middle (i.e., the northern LBB; Tournadour, 2015; Chabaud et al., 2015; Chabaud, 2016; Fauquembergue et al., 2018) to lower slopes (i.e., the eastern LBB; Recouvreur et al., 2020), or (b) contourites deposited or reworked by

deep contour currents (e.g., northern margin of the GAC, the Nares abyssal plain (Eberli & Betzler, 2019; Fauquembergue et al., 2023; Mulder et al., 2019; Recouvreur et al., 2020).

The predominance of hyperboles generally coincides with two types of surfaces: (a) a strongly indurated seabed or (b) the flanks of steep slopes. The indurated surfaces occur in areas influenced by the Florida Current or the Antilles Current (lower slope of the LBB), which mostly flow at water depths around 1,000 m. The map shown in Figure 4 illustrates the complexity of the deposits observed along the Bahamian slopes as well as the extent of the

factors that control sediment deposition during the Quaternary period in this area (Figure 5). For example, the northern LBB margin and the western GBB margin both present a similar echofacies distribution (Figure 5); the upper and middle slopes show bedded deposits rich in platform-derived particles. The lower slope displays numerous indurated nodules (Dix & Mullins, 1988; Schlager & James, 1978) associated with low sedimentation rates (and enhanced diagenesis) and increasing influence of currents with depth that is to say the increased intensity of the Antilles and Florida currents in the lower slope environment. These currents also limit the depth extension of facies related to platform export that never exceed 2,000 m deep and few kilometers away from the coastline, but allow the development of contourite drifts (Figure 1).

5.4. Quaternary Sedimentation Patterns

Acoustic results obtained on reflectivity, bathymetry and echofacies highlight large-scale similarities between slopes at the Bahamas. However, the analysis of detailed Quaternary grain-size partitioning highlights various differences for the individual slopes. For example, the coarse-grained mud-poor sequences are mainly concentrated on three environments:

1. The abyssal plain of San Salvador where the fan associated with the Exuma Canyon ends and where coarse turbidite deposits are frequent that disrupt the hemipelagic deposits supplied by the DWBC (Cartwright, 1985; Droxler, 1984; Le Goff et al., 2021).
2. The northern margin of the LBB where coarse sediment layers were deposited through large-scale gravity displacement events during MIS 5 similar to the ones found on Exuma Sound records (Crevello & Schlager, 1980; Reijmer et al., 2015; Spence & Tucker, 1997).
3. In the turbidite lobes located on the north-eastern LBB margin (Fauquembergue et al., 2023; Recouvreur et al., 2020).

Other variations in grain size were discussed by Rendle-Bühning and Reijmer (2005), who analyzed the grain-size evolution of the leeward and windward sides of the GBB up to MIS 21 (900 ka) and highlighted that coarse-grains are more common on leeward slopes during glacial periods, as they show an increase on the windward slopes during interglacial periods. This difference between the leeward and windward slopes is due to different sediment processes implied in both leeward and windward situations, with platform productivity export dominated by carbonate mud influencing the leeward margins and gravity-induced re-sedimentation processes prevailing at the windward margins.

Mud is more easily mobilized than coarse-grained sediments. The predominance of fine-grained sediment export from platforms to slopes could be explained by the large amount of fine mud material covering the interior of the banks (Figure 1). Recent studies have discussed that wind-induced currents and waves cause sediment suspension across the leeward margin of the GBB as tidal currents dominate this process along the wind-dominated GBB margin (Lopez-Gamundi et al., 2023). Hence, wind-induced currents and waves move the mud easily toward the platform edges, forming peri-platform ooze wedges present at the different margins (Chabaud, 2016; Chabaud et al., 2015; Droxler, 1984; Fauquembergue et al., 2018; Lantzsch et al., 2007; Roth & Reijmer, 2004, 2005; Wilber et al., 1990). Mud accumulation will impact slope angles that drive gravity processes on lower slopes (Figure 7; Kenter, 1990) as middle and lower slopes are affected by contour currents that may limit sediment deposition and even induce erosion within those areas (Chabaud, 2016; Rendle & Reijmer, 2002; Schlager & Ginsburg, 1981).

5.5. Main Factors Influencing Bahamian Slopes Morphology: Large Scale to Sample Scale Variations

Figure 6 shows the different domains and structures observed along the Bahamian slopes. Figure 7 provides a summary of the Quaternary sedimentary processes for (a) the slopes east of the Cay Sal Bank, (b) south-western GBB (Santaren Channel; Wunsch et al., 2016, 2018), (c) east of the GBB (Florida Straight; Principaud et al., 2015, 2017, 2018), (d) Exuma Sound and its canyon (Cartwright, 1985; Crevello & Schlager, 1980), and (e) the northern slope of LBB.

Three kinds of structures dominate the Bahamian slope morphologies (Figures 6 and 7): (a) structures related to sediment export from the shelves toward the deeper slopes as expressed by gullies, canyons, channeled lobes, turbidite fans, a channel-levee complex, and distributary furrows, (b) structures linked to sediment failure as

marked by platform margin collapse, slide scars and MTC, and (c) structures associated with current activity notably drifts, dunes and furrows and carbonate mounds.

Canyons connecting lower slopes to abyssal plains are structurally controlled by greater fracture intensity (Mulder et al., 2018; Recouvreur et al., 2020) in contrast to the canyons that export platform sediments to the lower slope. Platform export (Figure 7) mainly consists of mud, but can locally include coarse-grained sediment like on the north-western LBB during the MIS 5 (Fauquembergue et al., 2023), the north-eastern LBB slope where it supplies lobes (Fauquembergue et al., 2023; Recouvreur et al., 2020), within Exuma Canyon where MTCs spatially evolve as debris flows, grain flows and turbidity currents (Crevello & Schlager, 1980; Reijmer et al., 1992) or within TOTO with turbidity currents positioned in several lobes (Droxler & Schlager, 1985; Haak & Schlager, 1989). The north-western LBB MTC does not present the same evolution as the Exuma Sound MTC as the slope angles in Exuma Sound are steeper (Figure 2), the basin is deeper, and the coarse grains are more concentrated within the upper Exuma platforms' facies. Thus, repartition of platform facies productivity, linked to sea level and energy flux, has an impact on the sediment type that is available for the platform to slope and basin export.

At the toe of the north-western LBB slide scar, some structures interpreted as cold-water coral mounds are observed (Tournadour et al., 2015). Cold-water coral mounds are often present in vigorous current areas. Surface and deep-water currents have a considerable impact on the sedimentary structures and associated deposits that developed during the Quaternary. Cold-water coral mounds occur widespread along the slopes of the Bahamas. They are not only frequently found on the northern slope of the LBB where they mix with pelagites, hemipelagites and contourites but also in the Santaren Channel (e.g., Correa et al., 2012; Lüdmann et al., 2016). Deeper on the slope, on the Blake Plateau, currents are strong enough to prevent deposition and induce northwest-southeast oriented erosion lineaments (Mulder et al., 2018). Thus, depositional areas and the quantity of pelagic supply on slopes along the carbonate margin are highly influenced by the intensity of the deep-sea currents.

Along the western leeward GBB slopes (Figures 6 and 7), platform export is particularly important and builds sedimentary structures such as sediment waves, channel-levee systems, or gullies during Quaternary highstands at sea level (Chabaud, 2016; Mulder et al., 2014; Wunsch et al., 2016). On the north-western windward LBB slope, sediment export is limited and hence, such sedimentary structures do not develop. On the northern LBB slope, bathymetric data show that the canyon morphologies vary following a west-east trend along the bank slope (Mulder et al., 2012). The changing parameters are canyon length and width, depth of incision and channel sinuosity, highlighting a regional tectonic tilt of the bank and the morphology of the GAC, structurally controlled and opening from east to west, is consistent with this tilt (Mulder et al., 2012; Recouvreur et al., 2020). It affects the slope profiles: the NW LBB (Figures 2 and 7) corresponds to a bypass area, while at the north-eastern LBB, an accretionary sequence develops. The process of retrogressive erosion by which the canyons develop (Tournadour et al., 2017) is proposed for the western part of the LBB and suggested in the eastern part.

This data summary displays the strong impact of (Figure 7): (a) platform facies (quantity of coarse- and fine-grained sediment supply), (b) ocean currents (drift, coral mounds and erosion) and (c) regional tectonic (impact slopes angles) processes on carbonate slopes morphologies and on sediment composition of the slope deposits marking them.

Carbonate platform facies distribution and the presence of reefs influence sediment export, which influences the morphology of slope canyons as demonstrated by Puga-Bernabéu et al. (2011, 2013) for the mixed Great Barrier Reef system. The northern LBB slope revealed that the extent of the individual platform facies realms also influences sediment supply to the slope (Fauquembergue et al., 2023), where sediments derived from Bahamian platforms are generally fine-grained, so variations in physical energy fluxes mostly mobilize mud in this area. The slopes of Exuma Sound display a mix of platform derived fine and coarse grains and open-ocean input, hence resulting in a fairly typical mix of periplatform ooze and gravity deposits (Reijmer et al., 1988; Rendle-Bühning & Reijmer, 2005; Reijmer et al., 2015). The basin floor of Exuma Sound and Exuma Canyon are generally associated with large quantities of coarse-grained particles (Crevello & Schlager, 1980; Cartwright, 1985; Mulder et al., 2019; Le Goff et al., 2021; Figure 7). These coarse-grained facies are also observed on the north-eastern slope of the LBB (Figure 7). For both locations, the upstream shelves are depleted in mud and slightly richer in packstones and grainstones than elsewhere (Figure 1). These observations confirm that (a) the dominant facies on the platform seem to be an important factor controlling the slope facies (Figure 5) and (b) the direction of physical energy fluxes have an important influence on platform-export and related slope sedimentation rates (Fauquembergue et al., 2018; Wilber et al., 1990). Thus, energy fluxes direction influence both (a) platform facies

distribution and (b) on platform export to slope on downstream depositional areas. These findings agree with the sedimentation patterns observed for the slopes of the Great Barrier Reef also influenced by platform facies (Puga-Bernabéu et al., 2011, 2013).

Long-term records of the mud rich leeward margins of the Bahamas, for example, since the Cretaceous on the northwestern GBB, allowed a lateral migration of 25 km laterally (Eberli & Ginsburg, 1987, 1989). Muddy carbonate sequences are more frequent than coarse-grained sequences on leeward-positioned Bahamian slopes and allow the development of structures that agree with frequent sediment transport (moats, sediment waves, gullies and channel-levee systems; Figure 7; Principaud et al., 2018). Most of these sedimentary structures are active during highstands, particularly during highstands with sea level higher than for the Holocene, because of the enhanced productivity on the shelves. The slopes on the leeward margins receive large quantities of mud (forming periplatform ooze), which reflects the upstream platform facies and thus is a very important factor conditioning slope sediment supply. Sequences rich in coarse-grained platform-derived particles are not frequent, but their input may form important deposits (large sediment lobes) and may produce large structures such as canyons and debris flows that do not depend primarily on the wind direction. The same holds for the gravity deposits in the basins surrounded by shallow-water areas (e.g., TOTO: Droxler & Schlager, 1985; Haak & Schlager, 1989; Exuma Sound: Reijmer et al., 1988).

Thus, during sea-level highstands, a combination of tectonic (tilting) and platform export controls the quantity of coarse-grained export from the platform to the slopes. Deeper on the slope, currents have an important impact on seafloor morphology and on the location where the fine grains will be deposited.

During platform emersion, productivity largely stops or is limited to the marginal terraces like those present along the north-western LBB (Fauquembergue, 2018; Rankey & Doolittle, 2012). During these periods, emersion is characterized by cementation and karstification on the exposed platform (e.g., Dravis, 1979, 1996), and by cemented intervals (presence of nodules) on the slopes (Chabaud et al., 2015; Eberli et al., 2002; Lantzsch et al., 2007). Sea-level falls have often been considered as a significant factor contributing to margin collapse (Busson et al., 2021; Jo et al., 2015; Mullins & Hine, 1989) and the formation of megabreccias within both ancient and modern carbonate margins (Le Goff et al., 2020; Principaud et al., 2015), and pore-water overpressure was recognized as the dominant factor of destabilizations associated to these deposits (Spence & Tucker, 1997). In the Bahamas, within the Exuma Sound, debris flows were recognized (Crevello & Schlager, 1980) during glacial/interglacial transitions (Reijmer et al., 2015) and the overpressure scenario and associated sediment redeposition for the Western GBB slope were modeled by Busson et al. (2021) and discussed by Mullins and Hine (1989), Jo et al. (2015), Principaud et al. (2015) and Le Goff et al. (2020). The Exuma Sound debris flows present within the cores (Le Goff et al., 2021; Mulder et al., 2019) explain the higher quantities of coarse-grained sediment collected within the San Salvador abyssal plain within the lobe located at the mouth of Exuma Canyon. Despite the fact that most of the cores comprise periplatform ooze and the grain-size analysis in general does not exceed the sand size, it is important to note that platform margins and slopes can be affected by large-scale collapse and grain flows during the past.

6. Conclusions

The study of modern slope morphology, together with the analysis of backscatter and associated subsurface echofacies variations at the scale of the multiple Bahamian slopes, highlights that along the slopes of Bahamian platform systems, factors influencing slope sedimentation are similar. However, the relative impact of each factor, for example, (a) upstream facies mostly conditioned by physical fluxes and the location of the islands on the margin, and (b) current intensity leads to different models and a large diversity in slope morphology and associated deposits. The slopes discussed in this study can be dominated by platform-derived supply of coarse-grained grains or by fine-grained supply depending on the upstream dominating facies. Muds are easily mobilizable and subsequently these mud-dominated slope morphologies are highly influenced by currents. Impacting the grain-size distribution and forming contour deposits. Our results suggest that slope angles, bioclastic platform-derived export and deep (hemi)pelagic supply are the main modern factors influencing slope supplies.

Therefore, to confirm the importance of above-highlighted factors, for the entire Bahamas, it will be important to fill the central part of the map, as this part is still lacking in-depth data. Hence, a detailed morphology study of the TOTO slopes deploying the tools used for other slopes (direct grain-size measurements on long cores, bathymetry and reflection data, etc.) could confirm both (a) the hypothesis of a platform-wide tilting that we proposed based

on the flattening depth observed along the slopes and (b) detail the factors and processes at the origin of sediment transfer from carbonate shelves to slope observed on a Quaternary timescale within the most likely sand-rich TOTO area, which is a minor facies on the slopes discussed in this study.

Data Availability Statement

ArcGIS software (version 10.6; developed and maintained by Esri) was used to produce the maps discussed in this article. The processed data that were used in this manuscript will not be available in a data repository as a private company (TOTAL) funded the acquisition of most of them. Feel free to contact the authors on this topic.

Acknowledgments

TOTAL Research and Development (Pau, France) sponsored this study. We would like to thank the collaborators who contributed to the elaboration of this study, especially the captains and crews of the research vessels from Ifremer (R/V Le Suroit and l'Atalante) and RSMAS (R/V F. G. Walton Smith) as well as the scientific team members, including Sebastian Lindhorst, who helped with the acquisition of the data during the various expeditions. We would also like to thank the two anonymous reviewers that have accepted to review this manuscript and highly enriched its content.

References

- Adams, E. W., & Kenter, J. A. M. (2013). So different, yet so similar: Comparing and contrasting siliciclastic and carbonate slopes. In K. Verwer, T. E. Playton, & P. M. (Eds.), *Deposits architecture and controls of carbonate margin, slope and basinal settings* (Vol. 105, pp. 14–25). SEPM Special Publication. <https://doi.org/10.2110/sepmsp.105.14>
- Andrews, J. E., Shepard, F. P., & Hurley, R. J. (1970). Great Bahama Canyon. *Geological Society of America Bulletin*, 81(4), 1061. [https://doi.org/10.1130/0016-7606\(1970\)81\[1061:GBC\]2.0.CO;2](https://doi.org/10.1130/0016-7606(1970)81[1061:GBC]2.0.CO;2)
- Austin Jr., J. A., Schlager, W., Palmer, A. A., et al. (Eds.) (1986). *Proceedings of the ocean drilling program, 101 initial reports, proceedings of the ocean drilling program*. Ocean Drilling Program. <https://doi.org/10.2973/odp.proc.ir.101.1986>
- Ball (1967). Carbonate sand bodies of Florida and the Bahamas. *SEPM Journal of Sedimentary Research*, 37. <https://doi.org/10.1306/74D7171C-2B21-11D7-8648000102C1865D>
- Bergman, K. L. (2005). Seismic analysis of paleocurrent features in the Florida Straits: Insight into the paleo-Florida current, upstream tectonics, and the Atlantic-Caribbean connection. *Miami Times*.
- Bergman, K. L., Westphal, H., Janson, X., Poiriez, A., & Eberli, G. P. (2010). Controlling parameters on facies geometries of the Bahamas, an isolated carbonate platform environment. In H. Westphal, B. Riegl, & G. P. Eberli (Eds.), *Carbonate depositional systems: Assessing dimensions and controlling parameters* (pp. 5–80). Springer. https://doi.org/10.1007/978-90-481-9364-6_2
- Betzler, C., Lindhorst, S., Eberli, G. P., Ludmann, T., Mobius, J., Ludwig, J., et al. (2014). Periplatform drift: The combined result of contour current and off-bank transport along carbonate platforms. *Geology*, 42(10), 871–874. <https://doi.org/10.1130/G35900.1>
- Betzler, C., & Reijmer, J. J. G. (2014). Report and preliminary results of R/V meteor cruise M95 CICARB-current impact on the facies and stratigraphy of the Bahamas carbonate platform. *METEOR-Berichte*, 95, 1–36. https://doi.org/10.2312/cr_m95
- Boss, S. K., & Neumann, A. C. (1993). Impacts of Hurricane Andrew on carbonate platform environments, northern Great Bahama Bank. *Geology*, 21(10), 897–900. [https://doi.org/10.1130/0091-7613\(1993\)021<0897:iohaoc>2.3.co;2](https://doi.org/10.1130/0091-7613(1993)021<0897:iohaoc>2.3.co;2)
- Bourrouilh-Le-Jan, F. (1990). *Diagenèse des carbonates de plates-formes, récifs et mangroves en Atlantique et Pacifique. Contrôle de la diagenèse par les variations thermo-glacio-sustatiqued'émersion-submersion: aragonite, calcite, dolomite*. Univ. P.-et-M.-Curie ParisVI.
- Busson, J. (2018). *Caractérisation et modélisation numérique des transferts gravitaires de la plate-forme au bassin en contexte carbonate*. Université de Bordeaux.
- Busson, J., Joseph, P., Mulder, T., Teles, V., Borgomano, J., Granjeon, D., et al. (2019). High-resolution stratigraphic forward modeling of a Quaternary carbonate margin: Controls and dynamic of the progradation. *Sedimentary Geology*, 379, 77–96. <https://doi.org/10.1016/j.sedgeo.2018.11.004>
- Busson, J., Teles, V., Mulder, T., Joseph, P., Guy, N., Bouziat, A., et al. (2021). Submarine landslides on a carbonate platform slope: Forward numerical modelling of mechanical stratigraphy and scenarios of failure precondition. *Landslides*, 18(2), 595–618. <https://doi.org/10.1007/s10346-020-01510-7>
- Bustos-Serrano, H., Morse, J. W., & Millero, F. J. (2009). The formation of whittings on the Little Bahama Bank. *Marine Chemistry*, 113(1–2), 1–8. <https://doi.org/10.1016/j.marchem.2008.10.006>
- Cartwright, R. A. (1985). *Provenance and sedimentology of carbonate turbidites from two deep sea fans, Bahamas*. University of Miami, Coral Gables, Florida.
- Chabaud, L. (2016). *Modèle stratigraphique et processus sédimentaires au Quaternaire sur deux pentes carbonatées des Bahamas (leeward et windward)*. Université de Bordeaux.
- Chabaud, L., Ducassou, E., Tournadour, E., Mulder, T., Reijmer, J. J. G., Conesa, G., et al. (2015). Sedimentary processes determining the modern carbonate periplatform drift of Little Bahama Bank. *Marine Geology*, 378, 213–229. <https://doi.org/10.1016/j.margeo.2015.11.006>
- Correa, T. B. S., Grasmueck, M., Eberli, G. P., Reed, J. K., Verwer, K., & Purkis, S. (2012). Variability of cold-water coral mounds in a high sediment input and tidal current regime, Straits of Florida: Cold-water coral mound variability. *Sedimentology*, 59(4), 1278–1304. <https://doi.org/10.1111/j.1365-3091.2011.01306.x>
- Crevello, P. D., & Schlager, W. (1980). Carbonate debris sheets and turbidites, Exuma Sound, Bahamas. *Journal of Sedimentary Research*, 50. <https://doi.org/10.1306/212f7b99-2b24-11d7-8648000102c1865d>
- Dierssen, H. M., Zimmerman, R. C., & Burdige, D. J. (2009). Optics and remote sensing of Bahamian carbonate sediment whittings and potential relationship to wind-driven Langmuir circulation. *Biogeosciences*, 6(3), 487–500. <https://doi.org/10.5194/bg-6-487-2009>
- Dix, G. R., & Mullins, H. T. (1988). Rapid burial diagenesis of deep-water carbonates: Exuma Sound, Bahamas. *Geology*, 16(8), 680–683. [https://doi.org/10.1130/0091-7613\(1988\)016<0680:rbodow>2.3.co;2](https://doi.org/10.1130/0091-7613(1988)016<0680:rbodow>2.3.co;2)
- Dravis, J. (1979). Rapid and widespread generation of recent oolitic hardgrounds on a high energy Bahamian platform, Eleuthera Bank, Bahamas. *Journal of Sedimentary Research*, 49, 195–207.
- Dravis, J. J. (1996). Rapidity of freshwater calcite cementation—implications for carbonate diagenesis and sequence stratigraphy. *Sedimentary Geology*, 107, 1–10. [https://doi.org/10.1016/s0037-0738\(96\)00063-2](https://doi.org/10.1016/s0037-0738(96)00063-2)
- Droxler, A. W. (1984). *Late Quaternary glacial cycles in the Bahamian deep basins and in the adjacent Atlantic Ocean*. Miami, Coral Gables, Florida.
- Droxler, A. W., & Schlager, W. (1985). Glacial versus interglacial sedimentation rates and turbidite frequency in the Bahamas. *Geology*, 13(11), 799–802. [https://doi.org/10.1130/0091-7613\(1985\)13<799:gvisra>2.0.co;2](https://doi.org/10.1130/0091-7613(1985)13<799:gvisra>2.0.co;2)
- Eberli, G., & Ginsburg, R. N. (1989). *Cenozoic progradation of northwestern Great Bahama Bank, a record of lateral platform growth and sea-level fluctuations* (Vol. 44, pp. 339–351). Spec. Publ. Soc. econ. Paleont. Miner. <https://doi.org/10.2110/pec.89.44.0339>

- Eberli, G. P., Anselmetti, F. S., Kroon, D., Sato, T., & Wright, J. D. (2002). The chronostratigraphic significance of seismic reflections along the Bahamas Transect. *Marine Geology*, 185(1–2), 1–17. [https://doi.org/10.1016/s0025-3227\(01\)00287-0](https://doi.org/10.1016/s0025-3227(01)00287-0)
- Eberli, G. P., & Betzler, C. (2019). Characteristics of modern carbonate contourite drifts. *Sedimentology*, 66(4), 1163–1191. <https://doi.org/10.1111/sed.12584>
- Eberli, G. P., & Ginsburg, R. N. (1987). Segmentation and coalescence of Cenozoic carbonate platforms, northwestern Great Bahama Bank. *Geology*, 15(1), 75. [https://doi.org/10.1130/0091-7613\(1987\)15<75:SACOC>2.0.CO;2](https://doi.org/10.1130/0091-7613(1987)15<75:SACOC>2.0.CO;2)
- Enos, P. (1974). Map of surface sediment facies of the Florida-Bahamas Plateau.
- Fabregas, N. (2017). *Analyse morphobathymétrique et sismique très haute résolution de deux canyons sur la pente profonde des Bahamas (Rapport de stage)*. ENSEGD.
- Fauquembergue, K. (2018). *Transferts sédimentaires sur une marge carbonatée moderne de la plate-forme à la plaine abyssale: marge nord de Little Bahama Bank, Bahamas*. Université de Bordeaux.
- Fauquembergue, K., Ducassou, E., Mulder, T., Hanquiez, V., Perello, M.-C., Poli, E., & Borgomano, J. (2018). Genesis and growth of a carbonate Holocene wedge on the northern Little Bahama Bank. *Marine and Petroleum Geology*, 96, 602–614. <https://doi.org/10.1016/j.marpetgeo.2018.05.013>
- Fauquembergue, K., Ducassou, E., Mulder, T., Reijmer, J. J. G., Borgomano, J., Recouvreur, A., et al. (2023). Quaternary sedimentary processes on the Bahamas: From platform to abyss. *Marine Geology*, 459, 107044. <https://doi.org/10.1016/j.margeo.2023.107044>
- GEBCO Bathymetric Compilation Group. (2020). The GEBCO_2020 Grid - A continuous terrain model of the global oceans and land. <https://doi.org/10.5285/A29C5465-B138-234D-E053-6C86ABC040B9>
- Glaser, K. S., & Droxler, A. (1991). High production and highstand shedding from deeply submerged carbonate banks, northern Nicaragua rise. *Journal of Sedimentary Petrology*, 61, 128–142. <https://doi.org/10.1306/d42676a4-2b26-11d7-8648000102c1865d>
- Haak, A. B., & Schlager, W. (1989). Compositional variations in calciturbidites due to sea-level fluctuations, late Quaternary, Bahamas. *Geologische Rundschau*, 78(2), 477–486. <https://doi.org/10.1007/BF01776186>
- Harris, P. M. M., Purkis, S. J., Ellis, J., Swart, P. K., & Reijmer, J. J. G. (2015). Mapping bathymetry and depositional facies on Great Bahama Bank. *Sedimentology*, 62(2), 566–589. <https://doi.org/10.1111/sed.12159>
- Harwood, G. M., & Towers, P. A. (Eds.) (1988). Seismic sedimentologic interpretation of a carbonate slope, north margin of Little Bahama Bank, Proceedings of the Ocean Drilling Program, *Ocean Drilling Program*. <https://doi.org/10.2973/odp.proc.sr.101.1988>
- Jo, A., Eberli, G. P., & Grasmueck, M. (2015). Margin collapse and slope failure along southwestern Great Bahama Bank. *Sedimentary Geology*, 317, 43–52. <https://doi.org/10.1016/j.sedgeo.2014.09.004>
- Johns, B. (2011). R/V Knorr Cruise KN-200-4 (Cruise report). Port Everglades, FL to Port Everglades, FL.
- Kaczmarek, S. E., Hicks, M. K., Fullmer, S. M., Steffen, K. L., & Bachtel, S. L. (2010). Mapping facies distributions on modern carbonate platforms through integration of multispectral Landsat data, statistics-based unsupervised classifications, and surface sediment data. *AAPG Bulletin*, 94(10), 1581–1606. <https://doi.org/10.1306/04061009175>
- Kenter, J. A. M. (1990). Carbonate platform flanks: Slope angle and sediment fabric. *Sedimentology*, 37(5), 777–794. <https://doi.org/10.1111/j.1365-3091.1990.tb01825.x>
- Lantzsch, H., Roth, S., Reijmer, J. J. G., & Kinkel, H. (2007). Sea-level related re-sedimentation processes on the northern slope of Little Bahama Bank (Middle Pleistocene to Holocene). *Sedimentology*, 54(6), 1307–1322. <https://doi.org/10.1111/j.1365-3091.2007.00882.x>
- Leaman, K. D., Vertes, P. S., Atkinson, L. P., Lee, T. N., Hamilton, P., & Waddell, E. (1995). Transport, potential vorticity, and current/temperature structure across Northwest Providence and Santaren Channels and the Florida Current off Cay Sal Bank. *Journal of Geophysical Research*, 100(C5), 8561–8569. <https://doi.org/10.1029/94JC01436>
- Le Goff, J., Recouvreur, A., Reijmer, J. J. G., Mulder, T., Ducassou, E., Perello, M., et al. (2021). Linking carbonate sediment transfer to seafloor morphology: Insights from Exuma Valley, the Bahamas. *Sedimentology*, 68(2), 609–638. <https://doi.org/10.1111/sed.12794>
- Le Goff, J., Slooman, A., Mulder, T., Cavailhes, T., Ducassou, E., Hanquiez, V., et al. (2020). On the architecture of intra-formational mass-transport deposits: Insights from the carbonate slopes of Great Bahama Bank and the Apulian Carbonate Platform. *Marine Geology*, 427, 106205. <https://doi.org/10.1016/j.margeo.2020.106205>
- Lopez-Gamundi, C., Barnes, B. B., Bakker, A. C., Harris, P., Eberli, G. P., & Purkis, S. J. (2023). Spatial, seasonal and climatic drivers of suspended sediment atop Great Bahama Bank. *Sedimentology*, 71(3), 769–792. <https://doi.org/10.1111/sed.13151>
- Lüdmann, T., Paulat, M., Betzler, C., Möbius, J., Lindhorst, S., Wunsch, M., & Eberli, G. P. (2016). Carbonate mounds in the Santaren Channel, Bahamas: A current-dominated periplatform depositional regime. *Marine Geology*, 376, 69–85. <https://doi.org/10.1016/j.margeo.2016.03.013>
- Masaferro, J. L., & Eberli, G. P. (1999). Chapter 7 Jurassic-cenozoic structural evolution of the southern great Bahama bank. In *Sedimentary Basins of the World* (pp. 167–193). Elsevier. [https://doi.org/10.1016/S1874-5997\(99\)80041-0](https://doi.org/10.1016/S1874-5997(99)80041-0)
- Mulder, T., Ducassou, E., Gillet, H., Hanquiez, V., Principaud, M., Chabaud, L., et al. (2014). First discovery of channel-levee complexes in a modern deep-water carbonate slope environment. *Journal of Sedimentary Research*, 84(11), 1139–1146. <https://doi.org/10.2110/jsr.2014.90>
- Mulder, T., Ducassou, E., Gillet, H., Hanquiez, V., Tournadour, E., Combes, J., et al. (2012). Canyon morphology on a modern carbonate slope of the Bahamas: Evidence of regional tectonic tilting. *Geology*, 40(9), 771–774. <https://doi.org/10.1130/G33327.1>
- Mulder, T., Ducassou, E., Hanquiez, V., Principaud, M., Fauquembergue, K., Tournadour, E., et al. (2019). Contour current imprints and contourite drifts in the Bahamian archipelago. *Sedimentology*, 66(4), 1192–1221. <https://doi.org/10.1111/sed.12587>
- Mulder, T., Gillet, H., Hanquiez, V., Ducassou, E., Fauquembergue, K., Principaud, M., et al. (2018). Carbonate slope morphology revealing a giant submarine canyon (Little Bahama Bank, Bahamas). *Geology*, 46(1), 31–34. <https://doi.org/10.1130/G39527.1>
- Mulder, T., Joumes, M., Hanquiez, V., Gillet, H., Reijmer, J. J. G., Tournadour, E., et al. (2017). Carbonate slope morphology revealing sediment transfer from bank-to-slope (Little Bahama Bank, Bahamas). *Marine and Petroleum Geology*, 83, 26–34. <https://doi.org/10.1016/j.marpetgeo.2017.03.002>
- Mullins, H. T., & Hine, A. C. (1989). Scalloped bank margins: Beginning of the end for carbonate platforms? *Geology*, 17(1), 30. [https://doi.org/10.1130/0091-7613\(1989\)017<0030:SBMBOT>2.3.CO;2](https://doi.org/10.1130/0091-7613(1989)017<0030:SBMBOT>2.3.CO;2)
- Mullins, H. T., Neumann, A. C., Wilber, R. J., Hine, A. C., & Chinburg, S. J. (1980). Carbonate sediment drifts in Northern Straits of Florida. *The American Association of Petroleum Geologists Bulletin*, 64, 1701–1717. <https://doi.org/10.1306/2f9196ed-16ce-11d7-8645000102c1865d>
- Principaud, M. (2015). *Morphologie, architecture et dynamique sédimentaire d'une pente carbonatée moderne: le Great Bahama Bank (Bahamas)*. Université de Bordeaux.
- Principaud, M. (2016). Synthèse sédimentaire sur les pentes carbonatées bahamiennes: pente ouest du Great Bahama Bank et pente nord du Little Bahama Bank (Vol. 96).
- Principaud, M., Mulder, T., Gillet, H., & Borgomano, J. (2015). Large-scale carbonate submarine mass-wasting along the northwestern slope of the Great Bahama Bank (Bahamas): Morphology, architecture, and mechanisms. *Sedimentary Geology*, 317, 27–42. <https://doi.org/10.1016/j.sedgeo.2014.10.008>

- Principaud, M., Mulder, T., Hanquiez, V., Ducassou, E., Eberli, G. P., Chabaud, L., & Borgomano, J. (2018). Recent morphology and sedimentary processes along the western slope of Great Bahama Bank (Bahamas). *Sedimentology*, 65(6), 2088–2116. <https://doi.org/10.1111/sed.12458>
- Principaud, M., Ponte, J.-P., Mulder, T., Gillet, H., Robin, C., & Borgomano, J. (2017). Slope-to-basin stratigraphic evolution of the northwestern Great Bahama Bank (Bahamas) during the Neogene to Quaternary: Interactions between downslope and bottom currents deposits. *Basin Research*, 29(6), 699–724. <https://doi.org/10.1111/bre.12195>
- Puga-Bernabéu, Á., Webster, J. M., Beaman, R. J., & Guilbaud, V. (2011). Morphology and controls on the evolution of a mixed carbonate–siliciclastic submarine canyon system, Great Barrier Reef margin, north-eastern Australia. *Marine Geology*, 289(1–4), 100–116. <https://doi.org/10.1016/j.margeo.2011.09.013>
- Puga-Bernabéu, Á., Webster, J. M., Beaman, R. J., & Guilbaud, V. (2013). Variation in canyon morphology on the Great Barrier Reef margin, north-eastern Australia: The influence of slope and barrier reefs. *Geomorphology*, 191, 35–50. <https://doi.org/10.1016/j.geomorph.2013.03.001>
- Purdy, E. G. (1963a). Recent calcium carbonate facies of the Great Bahama Bank. 1. Petrography and reaction groups. *The Journal of Geology*, 71(3), 334–355. <https://doi.org/10.1086/626905>
- Purdy, E. G. (1963b). Recent calcium carbonate facies of the Great Bahama Bank. 2. Sedimentary facies. *The Journal of Geology*, 71(4), 472–497. <https://doi.org/10.1086/626920>
- Purkis, S., Cavalcante, G., Rohrla, L., Oehlert, A. M., Harris, P., & Swart, P. K. (2017). Hydrodynamic control of whittings on Great Bahama Bank. *Geology*, 45(10), 939–942. <https://doi.org/10.1130/G39369.1>
- Purkis, S. J., Harris, P., & Cavalcante, G. (2019). Controls of depositional facies patterns on a modern carbonate platform: Insight from hydrodynamic modeling. *Depositional Rec*, 5(3), 421–437. <https://doi.org/10.1002/dep.261>
- Rankey, E. C., & Doolittle, D. F. (2012). Geomorphology of carbonate platform–marginal uppermost slopes: Insights from a Holocene analogue, Little Bahama Bank, Bahamas: Uppermost carbonate platform slope, Bahamas. *Sedimentology*, 59(7), 2146–2171. <https://doi.org/10.1111/j.1365-3091.2012.01338.x>
- Recouvreux, A. (2017). *Analyse de la morphobathymétrie, des données acoustiques et de la sismique Très Haute Résolution du canyon d'Exuma (Bahamas) (Mémoire de Master - Université d'Aix Marseille)*. Université de Bordeaux. Labrotatoire EPOC.
- Recouvreux, A., Fabregas, N., Mulder, T., Hanquiez, V., Fauquembergue, K., Tournadour, E., et al. (2020). Geomorphology of a modern carbonate slope system and associated sedimentary processes: Example of the giant Great Abaco Canyon, Bahamas.
- Reijmer, J. J., Palmieri, P., Groen, R., & Floquet, M. (2015). Calciturbidites and calcidebrites: Sea-level variations or tectonic processes? *Sedimentary Geology*, 317, 53–70. <https://doi.org/10.1016/j.sedgeo.2014.10.013>
- Reijmer, J. J., Schlager, W., & Droxler, A. W. (1988). Site 632: Pliocene–Pleistocene sedimentation cycles in a Bahamian basin. In *The program, proceedings of the Ocean drilling program, scientific results leg 101. Ocean drilling program, College Station (TX)* (pp. 213–220).
- Reijmer, J. J. G., Schlager, W., Bosscher, H., Beets, C. J., & McNeill, D. F. (1992). Pliocene/Pleistocene platform facies transition recorded in calciturbidites (Exuma Sound, Bahamas). *Sedimentary Geology*, 78(3–4), 171–179. [https://doi.org/10.1016/0037-0738\(92\)90017-L](https://doi.org/10.1016/0037-0738(92)90017-L)
- Reijmer, J. J. G., Swart, P. K., Bauch, T., Otto, R., Reuning, L., Roth, S., & Zechel, S. (2009). A re-evaluation of facies on great Bahama Bank I: New facies maps of western Great Bahama Bank. In P. K. Swart, G. P. Eberli, J. A. McKenzie, I. Jarvis, & T. Stevens (Eds.), *Perspectives in carbonate geology* (pp. 29–46). John Wiley and Sons, Ltd. <https://doi.org/10.1002/9781444312065.ch3>
- Rendle, R. H., & Reijmer, J. J. G. (2002). Quaternary slope development of the western, leeward margin of the Great Bahama Bank. *Marine Geology*, 185(1–2), 143–164. [https://doi.org/10.1016/S0025-3227\(01\)00294-8](https://doi.org/10.1016/S0025-3227(01)00294-8)
- Rendle-Bühning, R. H., & Reijmer, J. J. G. (2005). Controls on grain-size patterns in periplatform carbonates: Marginal setting versus glacio-eustasy. *Sedimentary Geology*, 175(1–4), 99–113. <https://doi.org/10.1016/j.sedgeo.2004.12.025>
- Roth, S., & Reijmer, J. J. G. (2004). Holocene Atlantic climate variations deduced from carbonate periplatform sediments (leeward margin, Great Bahama Bank): Holocene Atlantic climate variations. *Paleoceanography*, 19(1). <https://doi.org/10.1029/2003PA000885>
- Roth, S., & Reijmer, J. J. G. (2005). Holocene millennial to centennial carbonate cyclicity recorded in slope sediments of the Great Bahama Bank and its climatic implications: Holocene carbonate cyclicity. *Sedimentology*, 52(1), 161–181. <https://doi.org/10.1111/j.1365-3091.2004.00684.x>
- Schlager, W., & Ginsburg, R. N. (1981). Bahama carbonate platforms—The deep and the past. *Marine Geology*, 44(1–2), 1–24. [https://doi.org/10.1016/0025-3227\(81\)90111-0](https://doi.org/10.1016/0025-3227(81)90111-0)
- Schlager, W., & James, N. P. (1978). Low-magnesian calcite limestones forming at the deep-sea floor, Tongue of the Ocean, Bahamas. *Sedimentology*, 25(5), 675–702. <https://doi.org/10.1111/j.1365-3091.1978.tb00325.x>
- Schlager, W., Reijmer, J. J. G., & Droxler, A. W. (1994). Highstand shedding of carbonate platforms. *SEPM Journal of Sedimentary Research*, 64B. <https://doi.org/10.1306/D4267FAA-2B26-11D7-8648000102C1865D>
- Schnyder, J. S. D., Eberli, G. P., Betzler, C., Wunsch, M., Lindhorst, S., Schiebel, L., et al. (2018). Morphometric analysis of plunge pools and sediment wave fields along western Great Bahama Bank. *Marine Geology*, 397, 15–28. <https://doi.org/10.1016/j.margeo.2017.11.020>
- Spence, G. H., & Tucker, M. E. (1997). Genesis of limestone megabreccias and their significance in carbonate sequence stratigraphic models: A review. *Sedimentary Geology*, 112(3–4), 163–193. [https://doi.org/10.1016/S0037-0738\(97\)00036-5](https://doi.org/10.1016/S0037-0738(97)00036-5)
- Thierry, M. (2010). CARAMBAR cruise, RV Le Suroît. <https://doi.org/10.17600/10020080>
- Toomey, M. R., Curry, W. B., Donnelly, J. P., & Hengstum, P. J. (2013). Reconstructing 7000 years of North Atlantic hurricane variability using deep-sea sediment cores from the western Great Bahama Bank. *Paleoceanography*, 28(1), 31–41. <https://doi.org/10.1002/palo.20012>
- Tournadour, E. (2015). Architecture et dynamique sédimentaire d'une pente carbonatée moderne: exemple de la pente Nord de Little Bahama Bank, Bahamas. Bordeaux.
- Tournadour, E., Mulder, T., Borgomano, J., Gillet, H., Chabaud, L., Ducassou, E., et al. (2017). Submarine canyon morphologies and evolution in modern carbonate settings: The northern slope of Little Bahama Bank, Bahamas. *Marine Geology*, 391, 76–97. <https://doi.org/10.1016/j.margeo.2017.07.014>
- Tournadour, E., Mulder, T., Borgomano, J., Hanquiez, V., Ducassou, E., & Gillet, H. (2015). Origin and architecture of a Mass Transport Complex on the northwest slope of Little Bahama Bank (Bahamas): Relations between off-bank transport, bottom current sedimentation and submarine landslides. *Sedimentary Geology*, 317, 9–26. <https://doi.org/10.1016/j.sedgeo.2014.10.003>
- US Naval Oceanographic Office. (1967). *Environmental atlas of the tongue of the ocean*. Bahamas (Special Publication No. SP-94).
- Vincent, R. (1981). BACAR cruise, RV Jean Charcot. <https://doi.org/10.17600/81002611>
- Wilber, R. J., Milliman, J. D., & Halley, R. B. (1990). Accumulation of bank-top sediment on the western slope of Great Bahama Bank: Rapid progradation of a carbonate megabank. *Geology*, 18(10), 970–974. [https://doi.org/10.1130/0091-7613\(1990\)018<0970:aobtso>2.3.co;2](https://doi.org/10.1130/0091-7613(1990)018<0970:aobtso>2.3.co;2)
- Wilson, P. A., & Roberts, H. H. (1992). Carbonate-periplatform sedimentation by density flows: A mechanism for rapid off-bank and vertical transport of shallow-water fines. *Geology*, 20(8), 713–716. [https://doi.org/10.1130/0091-7613\(1992\)020<0713:cpsbdf>2.3.co;2](https://doi.org/10.1130/0091-7613(1992)020<0713:cpsbdf>2.3.co;2)
- Wilson, P. A., & Roberts, H. H. (1995). Density cascading: Off-shelf sediment transport, evidence and implications, Bahama Banks. *SEPM Journal of Sedimentary Research*, 65A. <https://doi.org/10.1306/D426801D-2B26-11D7-8648000102C1865D>

- Wunsch, M., Betzler, C., Eberli, G. P., Lindhorst, S., Lüdmann, T., & Reijmer, J. J. G. (2018). Sedimentary dynamics and high-frequency sequence stratigraphy of the southwestern slope of Great Bahama Bank. *Sedimentary Geology*, *363*, 96–117. <https://doi.org/10.1016/j.sedgeo.2017.10.013>
- Wunsch, M., Betzler, C., Lindhorst, S., Lüdmann, T., & Eberli, G. P. (2016). Sedimentary dynamics along carbonate slopes (Bahamas archipelago). *Sedimentology*, *64*(3), 631–657. <https://doi.org/10.1111/sed.12317>
- Wylie Poag, C. (1991). Rise and demise of the Bahama-Grand Banks gigaplatform, northern margin of the Jurassic proto-Atlantic seaway. *Marine Geology*, *102*(1–4), 63–130. [https://doi.org/10.1016/0025-3227\(91\)90006-P](https://doi.org/10.1016/0025-3227(91)90006-P)
- Yao, Y., Hu, C., & Barnes, B. B. (2023). Mysterious increases of whitening events in the Bahama Banks. *Remote Sensing of Environment*, *285*, 113389. <https://doi.org/10.1016/j.rse.2022.113389>